DOI: 10.1002/asia.201000541

Total Synthesis and Biological Evaluation of a Series of Macrocyclic Hybrids and Analogues of the Antimitotic Natural Products Dictyostatin, Discodermolide, and Taxol

Ian Paterson,*[a] Guy J. Naylor,[a] Nicola M. Gardner,[a] Esther Guzmán,[b] and Amy E. Wright[b]

Dedicated to Professor Eiichi Nakamura on the occasion of his 60th birthday

Abstract: The design, synthesis, and biological evaluation of a series of hybrids and analogues of the microtubule-stabilizing anticancer agents dictyostatin, discodermolide, and taxol is described. A 22-membered macrolide scaffold was prepared by adapting earlier synthetic routes directed towards dictyostatin and discodermolide, taking advantage of the distinctive structural and stereochemical similarities between these two polyketide-derived marine natural products. Initial endeavors towards accessing novel discodermolide/dictyostatin hybrids led to the adoption of a late-stage diversification strategy and the construction of a small library of methyl-ether derivatives, along with the first triple hybrids bearing the side-chain of taxol or taxotere attached through an ester linkage. Biological assays of the anti-proliferative activity of these compounds in a series of human cancer cell lines, including the taxol-resistant NCI/ADR-Res cell line, allowed the proposal of various structure–activity relationships. This led to the identification of a potent macrocyclic discodermolide/dictyostatin hybrid **12** and its C9 methoxy derivative **38**, accessible by an efficient total synthesis and with a similar biological profile to dictyostatin.

Keywords: cytotoxicity · hybrids · natural products · total synthesis · tubulin

Introduction

Cancer is one of the leading causes of mortality in the developed world and its increasing prevalence highlights the compelling need to generate new and more effective therapies. One of the most promising avenues of cancer research is the study of natural products that attenuate cell growth by acting as inhibitors of cellular microtubules.[1] These compounds fall into two distinct groups: those that inhibit the assembly of tubulin heterodimers into microtubule polymers and those that stabilize microtubules.[2] These latter microtubule-stabilizing agents (MSA) impede the depolymerization of microtubules into their dimeric α,β-tubulin subunits, thereby preventing mitosis owing to stabilization of the mitotic spindle, thus leading to a block in the cell cycle at the G2/M phase and cell death by apoptosis.

The diterpenoid compound taxol (paclitaxel, **1**) was first isolated in 1962 from the Pacific Yew tree *Taxus Brevifolia* and was the first MSA to be discovered.[3] However, its biological mode of action remained unresolved for nearly two decades until Horwitz and co-workers revealed their seminal findings in 1979.[4] Since gaining FDA approval in 1992, taxol and subsequently its semisynthetic analogue taxotere (docetaxel, **2**)[5] have experienced widespread clinical use in a range of oncology treatments, including breast, ovarian, and lung cancers. Although the taxane class of cytotoxic drugs have great utility as chemotherapeutic agents, they suffer from low aqueous solubility and a tendency for drug resistance to develop in patients, further underlining the continued need for the identification of new microtubule-stabilizing agents.[6] This need has led to the search for structurally novel natural product scaffolds that share the same mode of action as the taxanes but have superior efficacy to

[a] Prof. Dr. I. Paterson, G. J. Naylor, Dr. N. M. Gardner
University Chemical Laboratory
Lensfield Road, Cambridge, CB2 1EW (UK)
Fax: (+44) 1223-336362
E-mail: ip100@cam.ac.uk
Homepage: http://www-paterson.ch.cam.ac.uk/

[b] Dr. E. Guzmán, Dr. A. E. Wright
Harbor Branch Oceanographic Institution at Florida Atlantic University, 5600 US 1 North, Fort Pierce, FL 34946 (USA)

Supporting information for this article is available on the WWW under http://dx.doi.org/10.1002/asia.201000541.

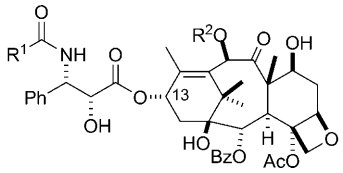

1: taxol (paclitaxel), R^1 = Ph, R^2 = Ac
2: taxotere (docetaxel), R^1 = *t*BuO, R^2 = H

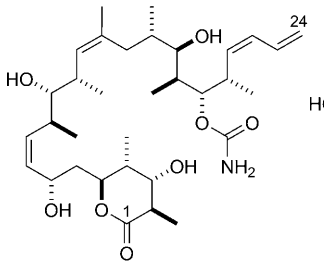

3: discodermolide

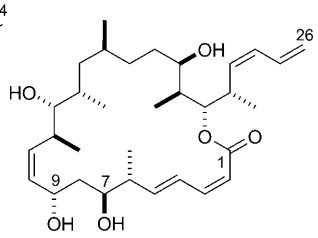

4: dictyostatin

overcome drug resistance. A major breakthrough was the discovery of the epothilones and the subsequent development of the semisynthetic lactam-derivative Ixempra as a clinically important anticancer drug.[7]

Discodermolide[8] (**3**) and dictyostatin[9] (**4**) are both marine sponge-derived polyketides that share the same microtubule-stabilizing mode of action as taxol. Significantly, they are poor substrates for the P-glycoprotein efflux pump and hence are able to maintain their antiproliferative ability against taxol-resistant cancer cell lines. Both discodermolide and dictyostatin are thought to bind at either the luminal taxoid binding site on β-tubulin or the recently discovered exterior pore site.[10] Assays also found the two drugs to have appreciably higher binding affinities than taxol; indeed discodermolide has the highest affinity of any known MSA,[11] and was also shown to have a synergistic relationship with taxol,[12] thus supporting their potential use together in combination therapies. Such promising anticancer properties have made discodermolide the focus of intensive synthetic and biological interest,[1d,13] culminating in the remarkable total synthesis of >60 g of this architecturally complex natural product for use in a Phase I clinical trial by Novartis,[14] for which unfortunately pulmonary toxicity issues arose.[15]

Key to understanding the cellular behavior of these compounds and crucial for the design of simplified and more potent analogues is the determination of their bioactive 3D conformations and their orientations within the taxoid binding site. To this end, numerous, and often conflicting, binding models have been postulated for taxol. Of the proposals, two preferred structures are "T-taxol"[16,17] and "REDOR-taxol".[18] Though broadly in agreement, a vigorous debate has since ensued as to the relative merits of these two viewpoints.[17,19]

As a lead structure for the generation of novel chemotherapeutic agents, discodermolide has also been a focus of extensive studies to elucidate the details of its binding interactions with β-tubulin and microtubules. The solid-state structure of discodermolide was resolved through X-ray crystallography to be "hairpin-like", in which the compound adopts a preorganized U-shaped conformation.[8a] The relative importance of this three-dimensional structure for solution and protein-bound environments has been hotly contested. However, a combination of NMR spectroscopic techniques and molecular modeling increasingly indicates that the hairpin structure is conserved across all three of these environments (Figure 1).[20,21] This distinctive conformational preorganization in discodermolide can be largely traced to the highly substituted propionate-derived backbone, with the minimization of *syn*-pentane steric interactions and A-(1,3)-strain about the $\Delta^{8,9}$ and $\Delta^{13,14}$ alkenes.[22]

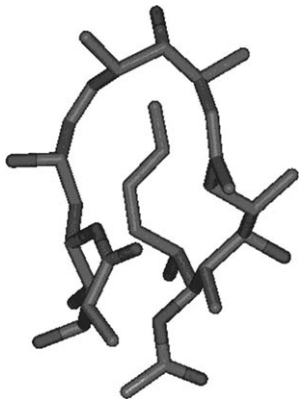

Figure 1. The lowest energy conformer of discodermolide in D_2O as deduced by Canales et al.[20] This hairpin conformation is broadly similar to the single-crystal X-ray structure of discodermolide in the solid state.

With respect to the orientation of the ligand within the protein binding pocket, there is still debate. Canales et al. used the AutoDock program to analyze the interactions of bioactive, conformationally-locked discodermolide with β-tubulin, and found that the compound sat exactly in the luminal taxoid binding site.[20] Snyder and co-workers re-examined this calculation by using the same discodermolide hairpin coordinates, but they employed three different docking programs.[23] They identified two distinct poses within the taxoid binding site, one of which matched the Canales binding model.

With intriguing structural similarities to discodermolide, the 22-membered macrolide dictyostatin has recently emerged as a new MSA with promising anticancer properties, and has been the focus of extensive synthetic and biological studies.[24] In an ambitious paper, Canales et al. proposed a unified binding model for discodermolide, dictyostatin, and taxol.[20] As previously described, the solution and tubulin-bound conformation of discodermolide were determined through NMR spectroscopic techniques and were found to be strikingly similar. However, the same methods when applied to dictyostatin revealed a profound difference in these structures, implying that a far higher degree of conformational selection is required during the binding event.

Significantly, the bound conformer of dictyostatin was discovered to closely resemble bound discodermolide, which suggests that the two compounds could potentially share the majority of their interactions with common amino acid residues of the protein. This supposition was further supported by the results of docking these bioactive conformations onto tubulin with AutoDock. Dictyostatin was found to occupy the taxoid site in a closely correlated pose to discodermolide, as can been seen in the overlaid image of the two ligands bound to β-tubulin (Figure 2).

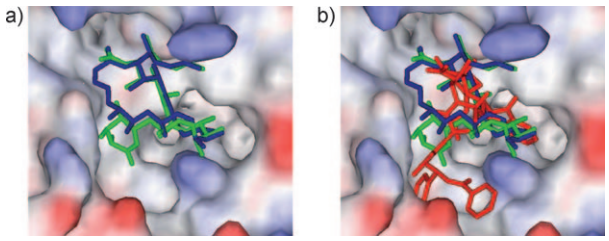

Figure 2. a) The microtubule-bound bioactive conformations of discodermolide (green) and dictyostatin (blue) overlaid at the taxoid binding site on β-tubulin, as calculated with AutoDock by Canales et al.[20] b) Taxol (red) has also been included; the additional region of the binding pocket exploited by the C13 ester side chain can be distinguished.

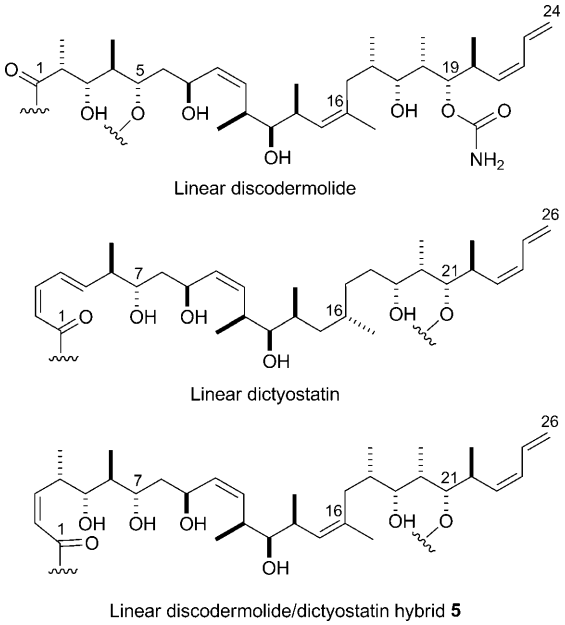

Scheme 1. Representations of the C1–C24 carbon chain of discodermolide (**3**) and the C1–C26 chain of dictyostatin (**4**) drawn in a linear manner to allow comparison of the matching stereochemistry and structural features, leading to the design of putative macrocyclic hybrid **5**.

Superimposition of all three MSAs at the taxoid site revealed that discodermolide and dictyostatin did not fully occupy the taxoid binding pocket. The two polyketides sit in the same region as the polycyclic baccatin core of taxol, but the C13 side-chain of taxol extends into a cleft of the binding site that is not exploited by either discodermolide or dictyostatin. Building on previous work on dictyostatin analogues by the Curran group and ourselves,[24] we sought to use the tubulin binding models proposed by Canales et al. as the basis for the rational design of hybrids between discodermolide and dictyostatin and, more speculatively, for a series of triple hybrids incorporating the taxol or taxotere side-chains.

Results and Discussion

Synthesis of Hybrids of Dictyostatin, Discodermolide, and Taxol

Prior to Canales et al. reporting their findings, as part of our on-going efforts to generate highly potent analogues of dictyostatin,[24h] we embarked on a synthesis of a first-generation discodermolide/dictyostatin hybrid.[25] Initial investigations were stimulated by their identical biological modes of action and the striking structural similarities between discodermolide and dictyostatin when the two linear carbon backbones are compared (Scheme 1). Encouraging initial findings on some simplified discodermolide/dictyostatin hybrids had been also been reported by the Curran group[24a] before the full configuration of dictyostatin had been determined.[9c]

At the outset, in-house molecular modeling had indicated that the lowest-energy conformer of discodermolide in water possessed the same hairpin geometry seen in the X-ray crystal structure and overlaid closely with the lowest-energy structure of the dictyostatin macrolide. This led to the design of the 22-membered macrolide structure **5** (Schemes 1 and 2), incorporating the full C2–C24 linear sequence of discodermolide and the (*Z*)-enoate of dictyostatin, leading to an extended C1–C26 carbon chain.[25] It was hypothesized that restricting the open chain structure of discodermolide into a macrocyclic motif, inspired by dictyostatin, would help in reducing any conformational selection that would be required for tubulin binding.

The retrosynthetic analysis for this initial hybrid **5** was heavily influenced by our previous endeavors towards achieving a practical and highly stereoselective synthesis of discodermolide, along with obtaining access to stocks of key advanced intermediates.[26] By following our second-generation total synthesis of discodermolide, a boron-mediated aldol reaction of ketone **6** and aldehyde **7** would be the centerpiece of the assembly of macrocyclic analogue **5**, employing a Yamaguchi macrolactonization[27] to close the 22-membered macrolactone.

Aldehyde **7** was conveniently accessed by a straightforward synthetic sequence (see the Supporting Information) from known diol **8**, which incorporates the required stereotriad configuration (Scheme 3).[26b,c] The more stereochemically elaborate ketone **6** was generated from bis(PMB) ether **9**, an advanced C13–C24 intermediate employed in our earlier discodermolide synthesis,[26a,b] by an efficient three-step sequence to install the (*Z*)-enone.[26d] Selective re-

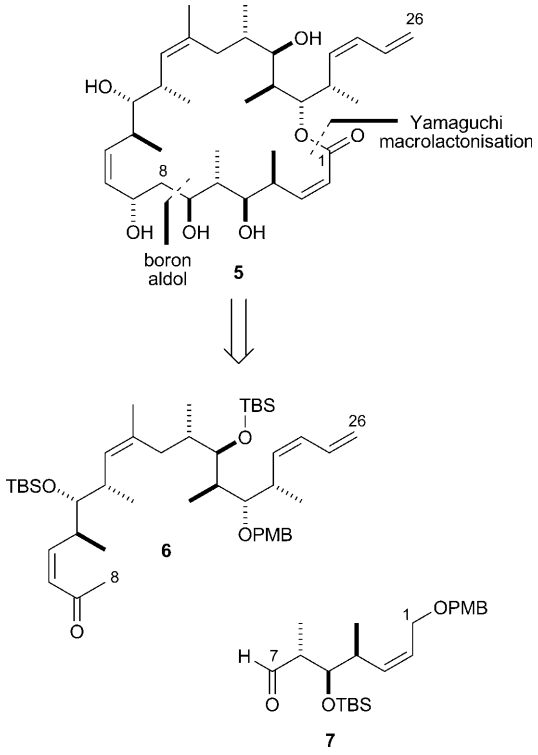

Scheme 2. Retrosynthetic analysis of dictyostatin/discodermolide hybrid **5**.

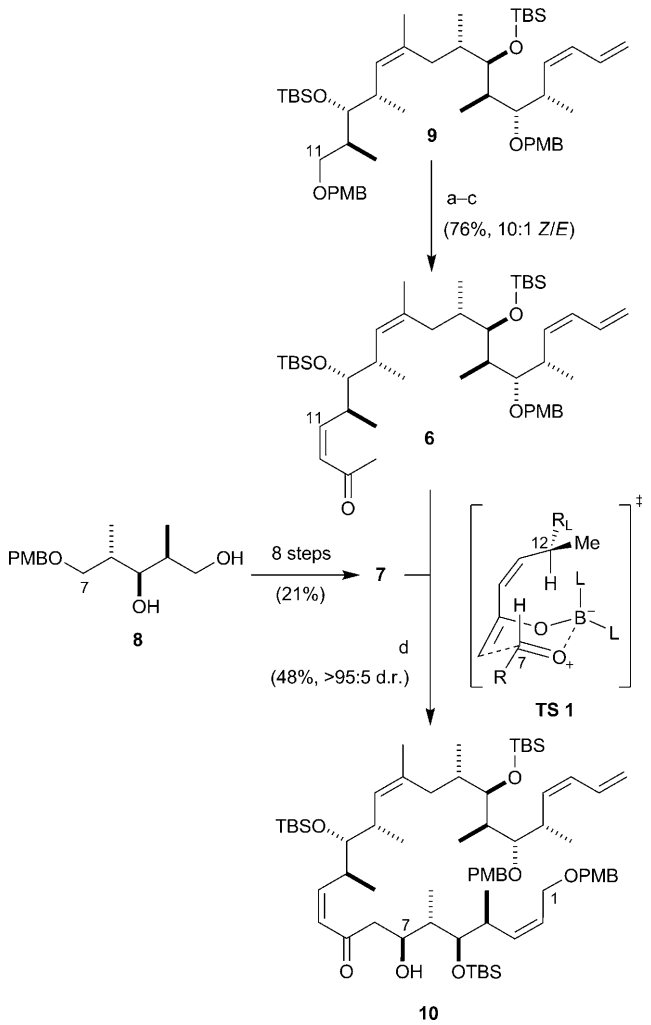

Scheme 3. Generation of aldol adduct **10**: a) BCl_3·DMS, CH_2Cl_2, −78→0 °C, 2 h; b) TEMPO, $PhI(OAc)_2$, CH_2Cl_2, 20 °C, 2 h; c) K_2CO_3, [18]crown-6, $(CF_3CH_2O)_2P(O)CH_2COMe$, PhMe/HMPA, 0 °C, 16 h; d) i) **6**, Et_3N, *c*-Hex_2BCl, Et_2O, 0 °C, 1 h; **7**, −78 °C, 15 min, ii) pH 7 buffer. DMS = dimethyl sulfide, HMPA = hexamethylphosphoramide, PMB = *p*-methoxybenzyl, TBS = *tert*-butyldimethylsilyl, TEMPO = 2,2,6,6-tetramethylpiperidine-1-oxy radical.

moval of the primary PMB ether was achieved on treatment of **9** with BCl_3·DMS,[28] followed by TEMPO/$PhI(OAc)_2$ oxidation[29] of the resulting alcohol to the aldehyde and Still–Gennari olefination[30] to afford **6** (10:1 *Z*/*E*). The two coupling partners were now subjected to the pivotal aldol reaction. Enolization of methyl ketone **6** with *c*-Hex_2BCl and Et_3N in ether at 0 °C led to the formation of the required boron enolate after 1 hour. Subsequent addition of an ethereal solution of aldehyde **7** at −78 °C and stirring for 15 minutes resulted in complete consumption of the limiting aldehyde partner to give aldol adduct **10** (48 %), with essentially complete diastereoselectivity at C7 (> 95:5 d.r. (d.r. = diastereomeric ratio)). The high level of stereocontrol with an *anti*-Felkin–Anh bias in this complex aldol coupling can be rationalized by invoking the preferred cyclic transition state **TS1**, and is consistent with our earlier work on exploiting 1,6-stereoinduction from structurally similar (*Z*)-enones in the context of our second-generation total synthesis of discodermolide.[26c,d]

After having formed the key C7–C8 bond, the complete C1–C26 carbon backbone of the hybrid was now in place. The endgame strategy commenced with setting the final C9 stereocenter by CBS reduction[31] of the enone, which afforded the desired 1,3-*anti* diol with useful stereoselectivity (75:25 d.r., Scheme 4). Acetonide protection and oxidative cleavage of both PMB ethers mediated by DDQ yielded the primary alcohol **11** (56 %). A two-step oxidation sequence generated the *seco*-acid, which underwent macrolactonization under modified Yamaguchi conditions[24c,32] (63 %). Finally, global deprotection (3 M HCl, MeOH) afforded the targeted discodermolide/dictyostatin hybrid **5**. Following HPLC purification, this initially designed hybrid construct was submitted to biological evaluation along with other synthetic analogues, as described later.

When planning our second-generation hybrid,[33] we had the additional benefit of being able to refer to the putative binding models proposed by Canales et al.[20] The structural similarities between discodermolide and dictyostatin coincide with the regions of greatest overlap, with the largest spatial discrepancies corresponding to the δ-lactone and dienoate functionalities. In designing the second-generation double hybrid **12**, we chose to furnish the regions of closest overlap (C8 to C26) with the discodermolide substitution pattern, whereas the region of greatest difference (C1 to C7) would be entirely dictyostatin-derived (Scheme 5). It

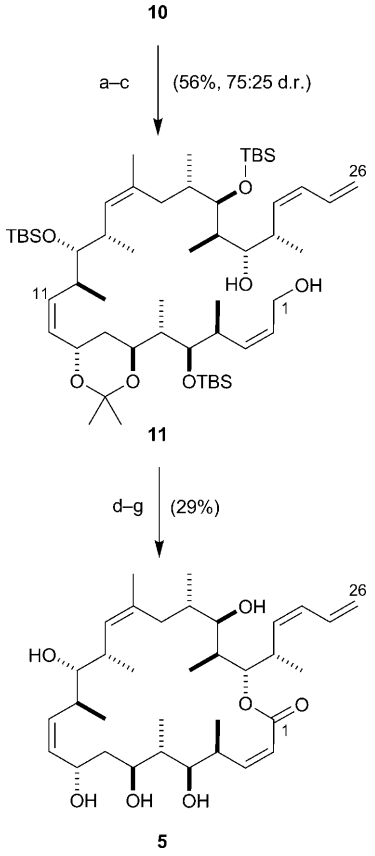

Scheme 4. Completion of hybrid **5**: a) (*R*)-CBS, BH_3·THF, CH_2Cl_2, 0 °C, 3 h; b) cat. PPTS, $(MeO)_2CMe_2$, 20 °C, 2 h; c) DDQ, CH_2Cl_2/pH 7 buffer, 20 °C, 3 h; d) cat. TEMPO, $PhI(OAc)_2$, CH_2Cl_2, 0→20 °C, 1 h; e) $NaClO_2$, NaH_2PO_4, 2-methyl-2-butene, *t*BuOH/H_2O, 20 °C, 4 h; f) 2,4,6-trichlorobenzoyl chloride, Et_3N, PhMe, 20 °C, 40 min; then DMAP, 20 °C, 20 min; g) 3 M HCl, MeOH, 0→20 °C, 8 h. CBS = Corey–Bakshi–Shibata catalyst, PPTS = pyridinium *para*-toluenesulfonate, DDQ = 2,3-dichloro-5,6-dicyano-1,4-benzoquinone, DMAP = 4-dimethylaminopyridine.

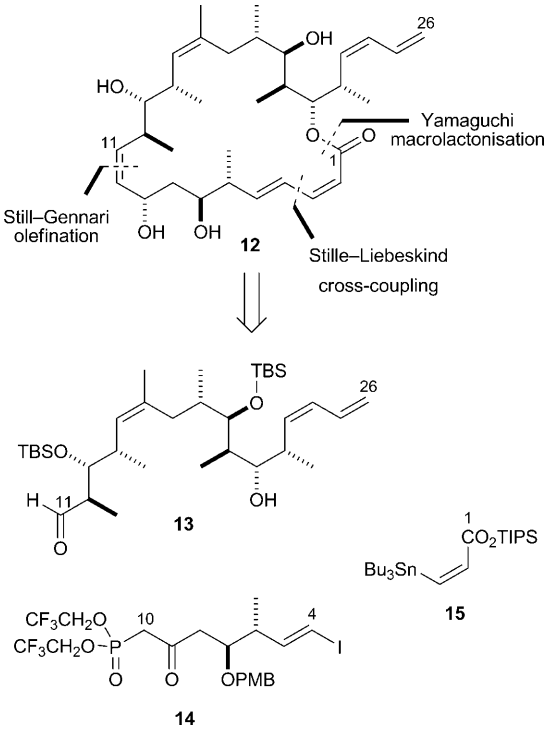

Scheme 5. Retrosynthetic analysis of discodermolide/dictyostatin hybrid **12**, leading to building blocks **13**, **14**, and **15**. TIPS = triisopropylsilyl.

was anticipated that the superior assembly inducing ability of dictyostatin[11] could, in part, be aided by the dienoate, and this might be reflected in the enhanced potency of this structurally more dictyostatin-like hybrid relative to **5**.

Our retrosynthetic analysis was also altered with respect to the initial hybrid **5**, with a cross-coupling-macrolactonization strategy preceded by an elaborate Still–Gennari olefination to unite the northern discodermolide hemisphere with the southern dictyostatin fragment. This would employ the highly functionalized β-ketophosphonate **14**, an intermediate initially developed for our second-generation total synthesis of dictyostatin.[34]

By employing the same optimized conditions as utilized for dictyostatin (K_2CO_3, [18]crown-6, PhMe/HMPA, 0 °C), the known aldehyde **13**[26a] and β-ketophosphonate **14** successfully underwent an olefination reaction on a gram scale to install the (*Z*)-alkene in 67 % isolated yield with 6.9:1 (*Z*:*E*) selectivity (Scheme 6). With enone **16** in hand, the remainder of the carbon backbone was rapidly assembled. As with the previous hybrid **5**, the most successful method for reducing the enone was under CBS conditions (> 95:5 d.r.), which was carried out subsequent to cleavage of the β-PMB ether (DDQ, 88 %) to achieve synthetically useful levels of selectivity. The success of this approach was in marked contrast to the poor conversion and low selectivity encountered under Evans–Saksena conditions.[35]

Acetonide protection proceeded smoothly (86 % over two steps), before a copper-mediated Stille–Liebeskind cross-coupling[36] between vinyl iodide **17** and stannane **15** completed the carbon backbone by installing the (2*Z*,4*E*)-dienoate. Macrolactonization under modified Yamaguchi conditions afforded the fully protected macrocycle, which was then deprotected (3 M HCl, MeOH) to provide hybrid **12** (72 %), with minimal translactonization onto the C19 hydroxyl. To further investigate the pharmacophore of this hybrid, and in particular the contribution of the C7,C9-diol, **12** was then treated with 2,2-dimethoxypropane and catalytic PPTS to reintroduce the acetonide to afford analogue **18**.

Taking inspiration from some of our earlier dictyostatin analogue work,[24e] the utility of the minor (*E*)-enone isomer obtained from the noteworthy Still–Gennari olefination giving **16** was explored. This late-stage intermediate could undergo selective conjugate reduction of the (10*E*)-enone and then be elaborated to a dihydro-analogue of hybrid **12**. Semisynthetic removal of the analogous olefin (along with several others) by catalytic hydrogenation of discodermolide to generate the reduced derivatives **19–21** had provided useful SAR insights (Scheme 7).[37] Furthermore, the 10,11-dihydro analogue **22** of dictyostatin was found to maintain its antiproliferative potency against most cancer cell lines,

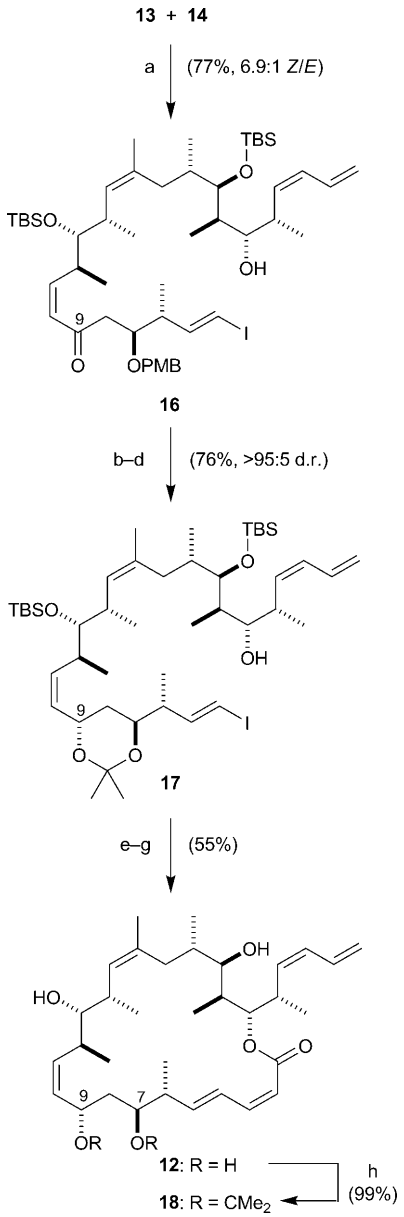

Scheme 6. Final steps leading to the discodermolide/dictyostatin hybrid **12** and acetonide **18**: a) **14**, K_2CO_3, [18]crown-6, PhMe/HMPA, 0 °C, 7 d; b) DDQ, CH_2Cl_2/pH 7 buffer, 0 °C, 2.5 h; c) (*R*)-CBS, BH_3·THF, THF, −30 °C, 36 h; d) PPTS, $(MeO)_2CMe_2$, CH_2Cl_2, 0→20 °C, 16 h; e) i) **15**, CuTC, NMP, 20 °C, 16 h; ii) KF, MeOH/THF, 20 °C, 90 min; f) 2,4,6-trichlorobenzoylchloride, Et_3N, PhMe, 20 °C, 1 h; DMAP, 20 °C, 4 d; g) 3 M HCl, MeOH, 0→20 °C, 16 h; h) PPTS, $(MeO)_2CMe_2$, 0→20 °C, 16 h. CuTC = copper(I)-thiophene-2-carboxylate, NMP = *N*-methylpyrrolidinone.

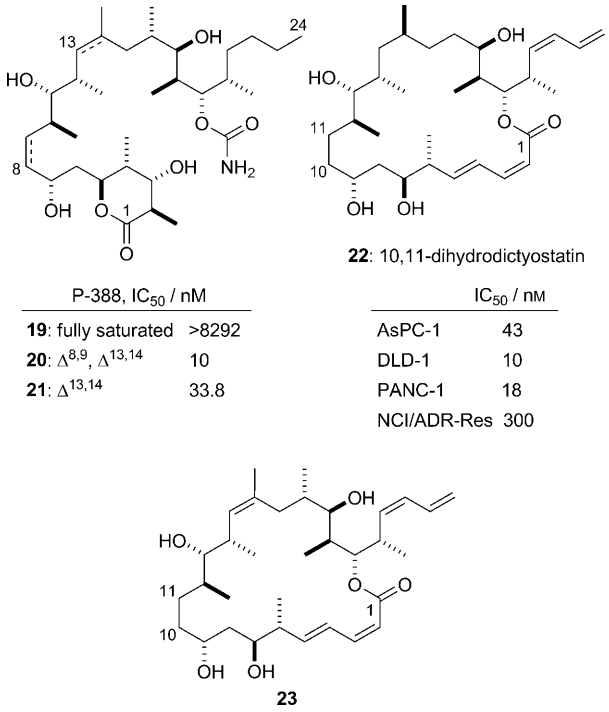

P-388, IC_{50} / nM	
19: fully saturated	>8292
20: $\Delta^{8,9}$, $\Delta^{13,14}$	10
21: $\Delta^{13,14}$	33.8

	IC_{50} / nM
AsPC-1	43
DLD-1	10
PANC-1	18
NCI/ADR-Res	300

Scheme 7. Reduced derivatives **19**, **20**, and **21** of discodermolide with various degrees of saturation and structures of 10,11-dihydro analogues **22** and **23** of dictyostatin and hybrid **12**, respectively.

with only moderate increases in IC_{50} values. There was a marked reduction in cytotoxicity against the taxol resistant NCI/ADR-Res cell line, however, implicating this olefin in playing a crucial role in avoiding an undesired protein residue contact with any mutations on β-tubulin, or in reducing its affinity for the P-glycoprotein efflux pump mechanism.

Analogue **23** would differ from the original 10,11-dihydrodictyostatin **22** by the additional methyl bearing stereocenter at C18 and the incorporation of a (*Z*)-trisubstituted olefin at C15–C16, with collateral loss of the C16 stereocenter. This additional hybrid was viewed as offering a useful contribution to the SAR data set for both dictyostatin and discodermolide.

Closely emulating our earlier work, conjugate reduction of enone **24** with freshly prepared Stryker's reagent[38] ($[Ph_3PCuH]_6$) provided the corresponding saturated ketone, which was then submitted to DDQ-mediated PMB deprotection (87%) to give diol **25** (Scheme 8). Whereas reduction of the analogous unsaturated β-hydroxy ketone precursor to hybrid **12** with (*R*)-CBS and BH_3·THF proved to be almost completely diastereoselective, on this substrate no useful selectivity was observed. Fortunately, Evans–Saksena conditions ($Me_4NBH(OAc)_3$, MeCN/AcOH, 2:1) also manifested the opposite behavior with **25** and now effected reduction with excellent levels of diastereoselectivity in favor of the desired 1,3-*anti* diol **26** (>95:5 d.r., 55% yield, 91% brsm). This outcome is rationalized by the previous CBS reduction experiencing a degree of matched substrate, as well as reagent stereocontrol, and saturation of the $\Delta^{10,11}$ olefin sufficiently alters the reacting conformation to remove this substrate bias, which may also have destabilized the normally preferred Evans–Saksena transition state.[39]

With the 1,3-*anti* diol **26** in hand, the synthesis of analogue **23** was completed in four steps (58%), by following the route taken earlier for hybrid **12**. The only slight modification being a reduction in the number of equivalents of DMAP in the macrocyclization step to minimize isomerism

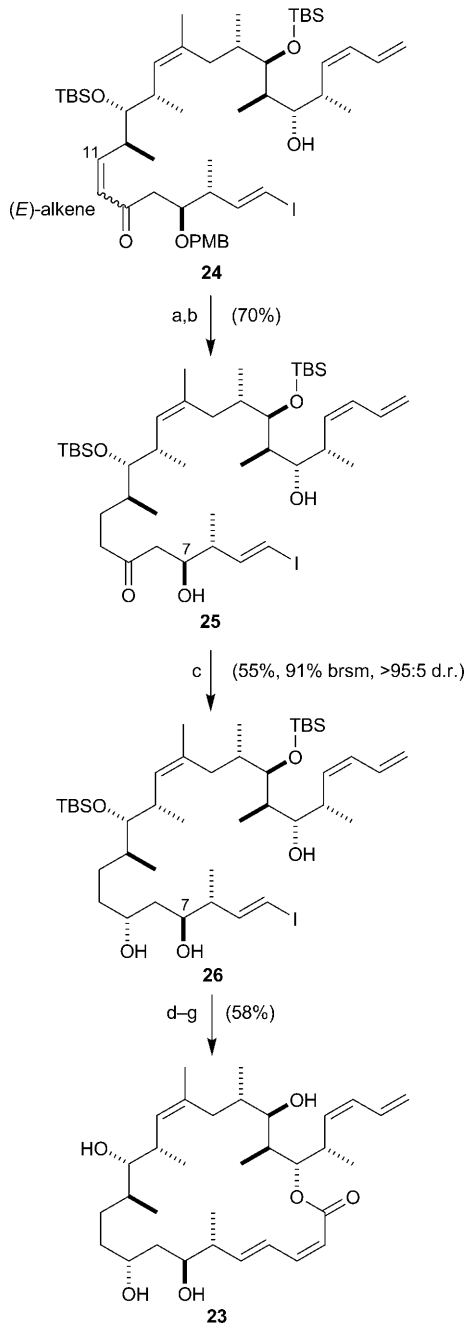

Scheme 8. Completion of 10,11-dihydro discodermolide/dictyostatin hybrid **23**: a) $[PPh_3CuH]_6$, PhMe/H_2O, 20 °C, 16 h; b) DDQ, CH_2Cl_2/pH 7 buffer, 0 °C, 2.5 h; c) $Me_4NBH(OAc)_3$, MeCN/AcOH, 0 °C, 16 h; d) PPTS, $(MeO)_2CMe_2$, CH_2Cl_2, 0→20 °C, 16 h; e) i) **15**, CuTC, NMP, 20 °C, 16 h; ii) KF, MeOH/THF, 20 °C, 2 h; f) 2,4,6-trichlorobenzoylchloride, Et_3N, PhMe, 20 °C, 1 h; then DMAP, 20 °C, 1 d; g) 3 M HCl, MeOH, 0→20 °C, 16 h.

of the (4*E*,2*Z*)-dienoate to the more thermodynamically favorable (4*E*,2*E*) configuration.[40]

As alluded to above, the unified binding model espoused by Canales et al. proposes that discodermolide and dictyostatin are located in the area of the binding site occupied by the baccatin core of taxol (Figure 2). In addition, the C13 side-chain of taxol occupies a further region of the pocket that is not taken advantage of by either of these polyketide structures. However, the C7 and C9 hydroxyls on dictyostatin are orientated to point into this unexploited pocket, and presumably this would also be true for double hybrid **12**. By appending the taxol or taxotere side chain onto either of these hydroxyls, it was hypothesized that additional binding interactions could be gleaned and in doing so generate the first triple hybrids.[41]

Taking advantage of fully protected macrolactone **27**, an advanced intermediate in the synthesis of hybrid **12**, a late-stage diversification strategy was pursued. Acetonide deprotection was affected with PPTS, MeOH/CH_2Cl_2 (1:1) to yield the 1,3-diol **28**, which would be the substrate for esterification (Scheme 9). Attachment of the side chains was achieved by following a modification of the original protocol developed to introduce the taxane side chain onto the C13 hydroxyl of baccatin III.[42] Accordingly, deprotonation of **28** with sodium bis(trimethylsilyl)amide (NaHMDS) followed by treatment with β-lactam **29** (taxol side chain, R = Ph) or **30** (taxotere side chain, R = O*t*Bu)[43] provided an inseparable mixture of regioisomeric esters. The ratio of C7 to C9 ester was found to be temperature dependent; for lactam **29** (R = Ph), the C9-coupled product dominated at 0 °C (2:1), whereas at lower temperatures, this selectivity was overturned and, surprisingly, the more sterically hindered C7 hydroxy was the favored reaction site (3:1). This mixture of esters was then deprotected under mild conditions (HF•py, pyridine) to yield the desired triple hybrids **31**–**34** that were separated by careful HPLC purification.

Attempted NMR spectroscopic characterization of these hybrids by using deuterated dimethyl sulfoxide (DMSO) and methanol brought to light several unexpected stability issues. Irrespective of the hybrid studied, dissolving in [D_6]DMSO resulted in the regiomerically pure hybrid undergoing tranesterification to produce an approximate 2:1 mixture of C9 to C7 esters. Upon heating, the bias towards the C9 regioisomer was further reinforced, presumably due to the more benign steric environment of this position. This result was especially notable as DMSO is commonly used as a solvent in biological assays, meaning any results could not be assumed to be for the pure compound. Intriguingly, after 72 hours in methanol solution, the side chains were found to be labile, reforming the original double hybrid **12** and the corresponding methyl ester derived from the taxol or taxotere side chain.

Drawing on findings from previous dictyostatin analogues prepared by our group, our attention was drawn to the highly potent 9-methoxydictyostatin derivative.[24c] In emulating this work, it was anticipated that by capping the C7 or C9 free hydroxyl as the methyl ether, we could prevent the undesired transesterification processes witnessed in dimethyl sulfoxide and methanol, without significantly altering the biological profile of the compounds.

Satisfyingly, treatment of diol **28** with Meerwein's salt and Proton Sponge was found to be highly regioselective (ca. 30:1) for the more nucleophilic C9 allylic alcohol (Scheme 10). The reaction time was found to be critical to

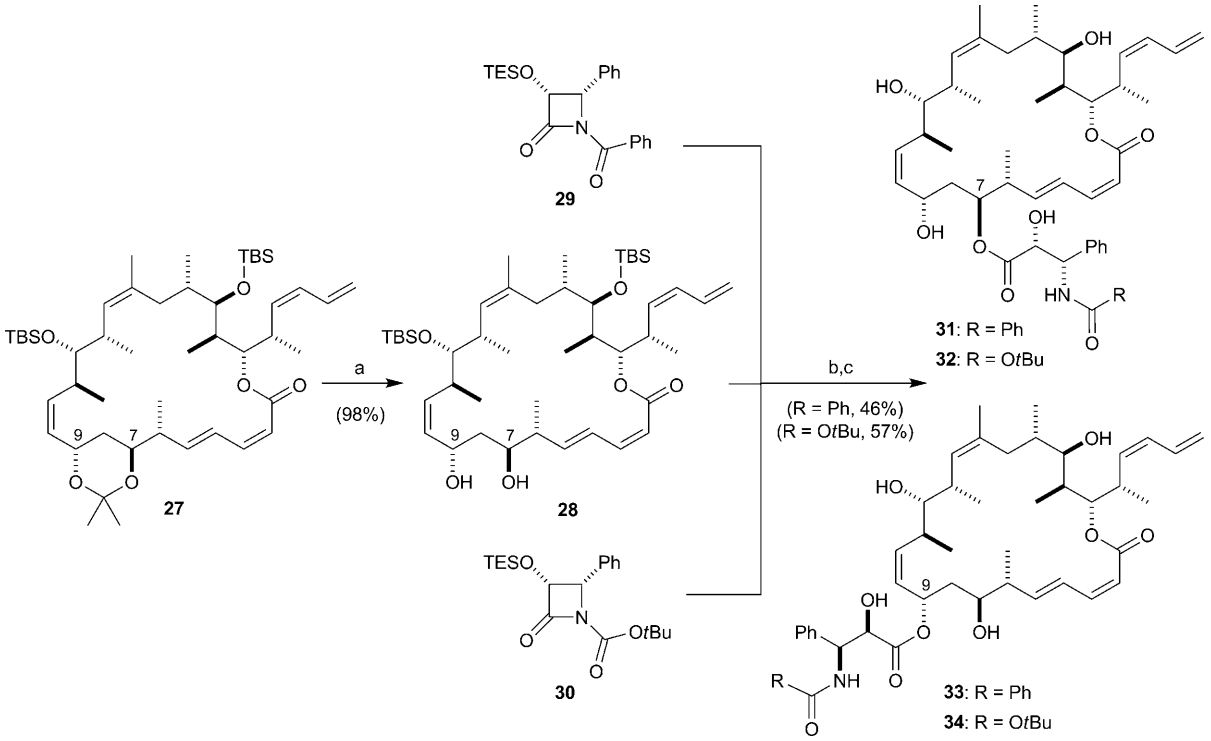

Scheme 9. Generation of triple hybrids **31**–**34**: a) PPTS, $MeOH/CH_2Cl_2$, 0→20 °C, 16 h; b) NaHMDS, THF, −78 °C, 10 min; **29** or **30**, −78→0 °C, 30 min; c) HF·py, pyridine, THF, 0→20 °C, 3 d. NaHMDS = sodium hexamethyldisilazide, TES = triethylsilyl.

preventing formation of the bis(methyl ether) **35**; typically the reaction had to be halted early and unreacted starting material recovered. However, sufficient quantities of **35** were isolated from initial reactions to be advanced to the C7,C9-dimethoxy derivative **36**. With the selectively methylated compound **37** in hand, deprotection with HF·py gave the novel C9 methoxy analogue **38**, whereas esterification with β-lactam **29** or **30** followed by subsequent deprotection gave esterified triple hybrids **39** and **40** (78 and 91 % yields over two steps, respectively).

A less direct approach would be necessary to access the corresponding C7 methoxy compounds. Continuing our strategy of late-stage diversification, the C9 hydroxy would first be selectively protected followed by C7−OH methylation and then C9 deprotection. This was achieved by treatment of 1,3-diol **28** with TESOTf and 2,6-lutidine in 71 % yield. Although this reaction proceeded in good regioselectivity (5:1 at −78 °C, further enhanced to >10:1 at −100 °C), bis(silylation) was also surprisingly facile (Scheme 11). Despite using only 1.1 equivalents of TESOTf, 17 % of **41** was generated as well as recovering 13 % of unreacted starting material. Consequently, the bis(TES) material was recycled back to diol **28** by a high-yielding PPTS, $MeOH/CH_2Cl_2$ deprotection (96 %) to minimize loss of material.

Reaction of mono-TES compound **42** with Meerwein's salt to cap the C7 free hydroxyl was then followed by selective cleavage of the TES group (99 %). At this stage, global deprotection led to the C7 methoxy analogue **44**, whilst treatment with NaHMDS and β-lactam **29** or **30** and subsequent deprotection gave O-methylated triple hybrids **45** and **46** (65 and 77 % yields over two steps, respectively).

Evaluation of the methyl ether triple hybrids **39**, **40**, **45**, and **46** demonstrated the successful elimination of all chemical stability issues. All compounds were found to be stable in dimethyl sulfoxide at ambient temperature for several weeks, and the side-chains were now unaffected by exposure to methanol. These results indicate that the neighboring free hydroxyl plays a decisive role in the transesterification of hybrids **31**–**34**.

Biological Evaluation

All of the prepared compounds were submitted to in vitro biological assays against at least two human cancer cell lines and their activities compared to taxol (**1**), discodermolide (**3**), and dictyostatin (**4**). The participating cell lines consisted of the AsPC-1 (pancreatic), DLD-1 (colon), PANC-1 (pancreatic), and NCI/ADR-Res (taxol-resistant ovarian), and all IC_{50} values quoted are the average from a minimum of three experiments (Table 1).

The most potent of the new compounds were the second-generation double hybrid **12** and its close structural derivative, the 9-methoxy analogue **38**, both displaying low nanomolar cytotoxicities in taxol-sensitive and -resistant cell lines. The moderate cytotoxicity of the initial discodermolide/dictyostatin hybrid **5** indicates that it is a much poorer antiproliferative agent than either of the two parent natural products, though it was still able to induce a G2/M block in

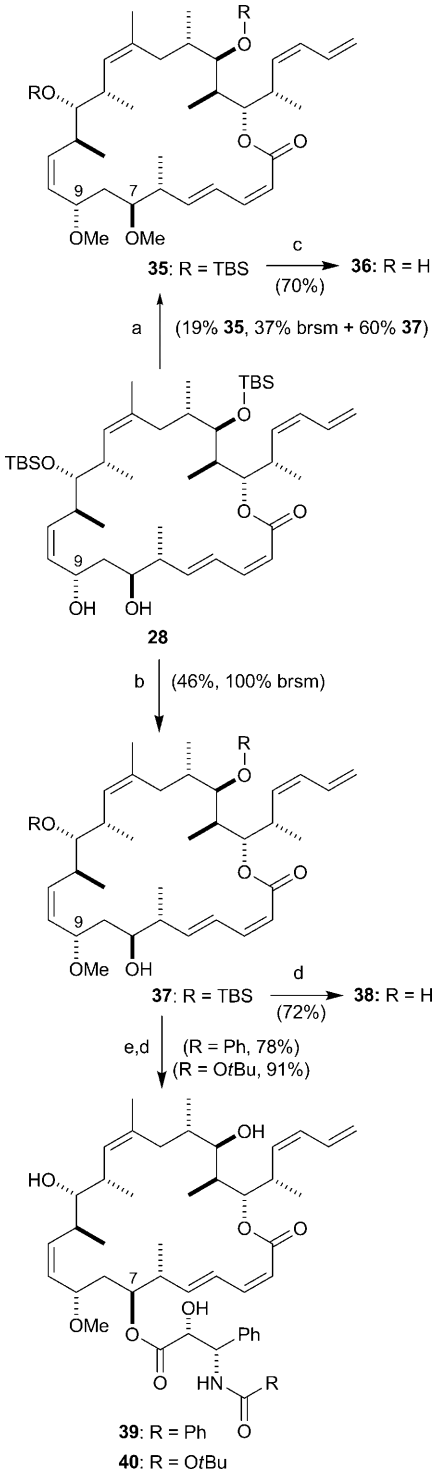

Scheme 10. Synthesis of C9-methoxy analogues **36** and **38**–**40**. a) $Me_3O{\cdot}BF_4$, Proton Sponge, CH_2Cl_2, 20 °C, 70 min; b) $Me_3O{\cdot}BF_4$, Proton Sponge, CH_2Cl_2, 20 °C, 45 min; c) 3 M HCl, MeOH, 0→20 °C, 16 h; d) HF·py, pyridine, THF, 0→20 °C, 3 d. e) NaHMDS, THF, −78 °C, 10 min; then **29** or **30**, −78→0 °C, 30 min.

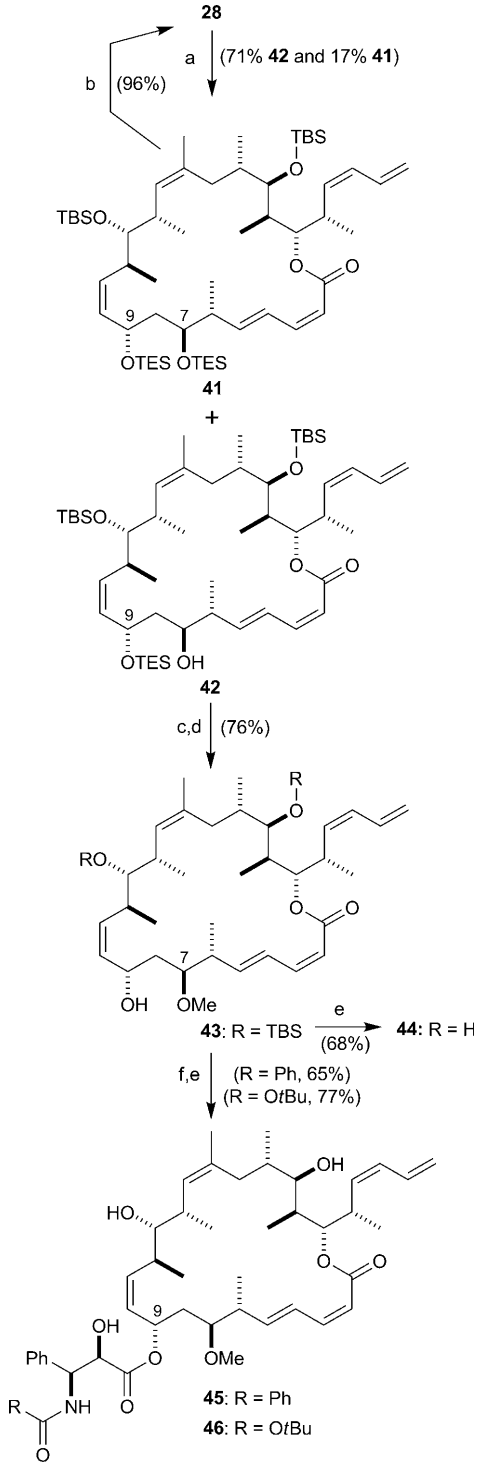

Scheme 11. Completion of the C7-methoxy analogues **44**–**46**: a) TESOTf, 2,6-lutidine, CH_2Cl_2, −98 °C, 90 min; b) PPTS, MeOH/CH_2Cl_2, 0→20 °C, 2 h; c) $Me_3O{\cdot}BF_4$, Proton Sponge, CH_2Cl_2, 20 °C, 90 min; d) PPTS, MeOH/CH_2Cl_2, 0→20 °C, 2 h; e) HF·py, pyridine, THF, 0→20 °C, 3 d; f) NaHMDS, THF, −78 °C, 10 min; then **29** or **30**, −78→0 °C. TESOTf = triethylsilyl trifluoromethanesulfonate.

cell cycle analysis assays. The structural differences between hybrids **5** and **12** (removal of substitution at C4 and C5 and replacement with an (*E*)-alkene) have a profound effect on cell growth inhibition capabilities. These alterations could allow **5** to access a disparate lowest-energy conformation that bears little similarity to the bioactive conformer, or it

Table 1. Cytotoxicity of taxol (**1**), discodermolide (**3**), dictyostatin (**4**), and all prepared analogues and hybrids in cultured human cancer cell lines.

Compound	IC_{50} [nM]			
	PANC-1 (pancreatic)	NCI/ADR-Res (ovarian)	AsPC-1 (pancreatic)	DLD-1 (colon)
taxol (**1**)	9.9 ± 1.3	1264 ± 141	149 ± 33	22 ± 1
discodermolide (**3**)	59 ± 34	160 ± 34	98 ± 34	29 ± 8
dictyostatin (**4**)	4.2 ± 0.5	6.6 ± 0.4	6.2 ± 0.6	2.2 ± 0.5
double hybrid **5**	1800	8200	2800	2100
double hybrid **12**	12 ± 2.0	66 ± 15	34 ± 6.4	6.0 ± 1.1
double hybrid **23**	138 ± 34	1450 ± 140	781 ± 100	130 ± 13
acetonide **18**	4860 ± 150	2930 ± 300	4830 ± 450	2350 ± 180
triple hybrid **31**	316 ± 56	4880 ± 420	–	–
triple hybrid **32**	181 ± 37	3090 ± 500	–	–
triple hybrid **33**	212 ± 45	2360 ± 100	–	–
triple hybrid **34**	224 ± 8.0	3250 ± 300	–	–
double hybrid **38**	17 ± 6.6	8.2 ± 4.3	–	–
double hybrid **44**	47 ± 2.8	380 ± 47	–	–
double hybrid **36**	60 ± 12	128 ± 11	–	–
triple hybrid **39**	293 ± 40	974 ± 14	–	–
triple hybrid **40**	190 ± 14	2040 ± 630	–	–
triple hybrid **45**	460 ± 50	2540 ± 450	–	–
triple hybrid **46**	412 ± 118	4400 ± 670	–	–

could be allowing unfavorable interactions to occur at the taxoid site. The satisfying biological results obtained for second-generation hybrid **12** (IC_{50} values intermediate between that measured for discodermolide and dictyostatin) acted as an incentive for its use as a lead compound for the generation of this diverse group of analogues and further hybrids. In analyzing the results for these compounds, some potential SAR trends have been identified.

The 10,11-dihydro analogue **23** was found to be at least one order of magnitude less active than its unsaturated equivalent **12**. This loss in activity was especially noticeable in the taxol-resistant NCI/ADR-Res cell line and broadly is in agreement with the behavior of 10,11-dihydro-dictyostatin **22**.[24e] The results for acetonide **18** are more enlightening when contrasted with those for 7,9-dimethoxy hybrid **36**. Analogue **18** has a relatively poor biological profile and does not cause an accumulation of cells at the G2/M block, whereas **36** is approximately equipotent with discodermolide. This suggests that neither of the C7,C9 hydroxyls are involved in stabilizing hydrogen-bonding interactions, and are probably not located in a sterically congested part of the binding site. However, the conformational rigidity imparted by the acetonide has a highly detrimental effect, potentially perturbing the bioactive conformation.

All of the triple hybrids **31**–**34** proved to be less cytotoxic than the parent double hybrid **12**, which demonstrated that the addition of the side chains did not lead to improved tubulin binding ability. Closer inspection also revealed a marked reduction in IC_{50} values for these hybrids (including the O-methylated derivatives), when comparing the PANC-1 results with those for NCI/ADR-Res. The presence of a taxane side chain appears to introduce limitations associated with the taxoid family. The values for the 7- and 9-taxotere hybrids **32** and **34** for both cell lines are surprisingly similar, and when taking into account the standard deviations, are virtually indistinguishable. This implies that the bioassay was actually performed on a mixture of regioisomers, the expected transesterification having arisen in the DMSO stock solution used to dissolve the compounds in preparation for testing. For the corresponding taxol hybrids **31** and **33**, the transesterification does not seem to have occurred to the same extent, as evidenced by the dissimilarity of their IC_{50} values. Upon comparing the different side chains, taxotere hybrids **32**, **34**, **40**, and **46** fared better in the pancreatic cell line, whereas their taxol counterparts **31**, **33**, **39**, and **45** performed more effectively in the taxol-resistant ovarian line (Figure 3).

Introduction of the methoxy functionality at the C7-position had a slightly negative impact, in particular for the NCI/ADR-Res cell line (interestingly, the dimethoxy congener **36** was more potent than **44** in this cell line). However, the 9-methoxy double hybrid **38** proved to be the most potent of all the synthesized compounds (with $IC_{50} = 8.2$ nM in the resistant NCI/ADR-Res cell line), approaching the IC_{50} values of dictyostatin itself. Furthermore, the 9-methoxy triple hybrids **39** and **40** were noticeably more active than the 7-methoxy hybrids **45** and **46**. In the cell cycle assays, C7-methoxy compound **44** caused 72% of the cell population to accumulate at the G_2/M block (PANC-1 treated with 100 nM of compound), whereas the C9-methoxy compound could manage an impressive 93%, matched exactly by the C7,C9-dimethoxy derivative (also 93%).

Conclusions

In summary, we have successfully designed and synthesized a series of novel hybrids of the antimitotic natural products dictyostatin, discodermolide, and taxol, which share a common microtubule stabilizing mode of action and tubulin binding site. The biological profile of the majority of these compounds is highly encouraging, with the discodermolide/dictyostatin hybrid **12** and its 9-methoxy derivative **38** especially worthy of note. These two compounds are now the focus of efforts to produce a quantity sufficient for in vivo testing. The triple hybrids, though displaying pleasing levels of cytotoxicity, did not lead to an increase in activity relative to the double hybrid **12** (contrast this with baccatin III and taxol). A number of factors could have contributed to this, including the increased polarity of the compounds now making them less cell permeable. The SAR trends revealed for these compounds will prove useful in the design of prospective taxol biomimetics and several of these active hybrid structures may provide molecular probes for exploring the molecular recognition details of the taxoid binding site on β-tubulin.

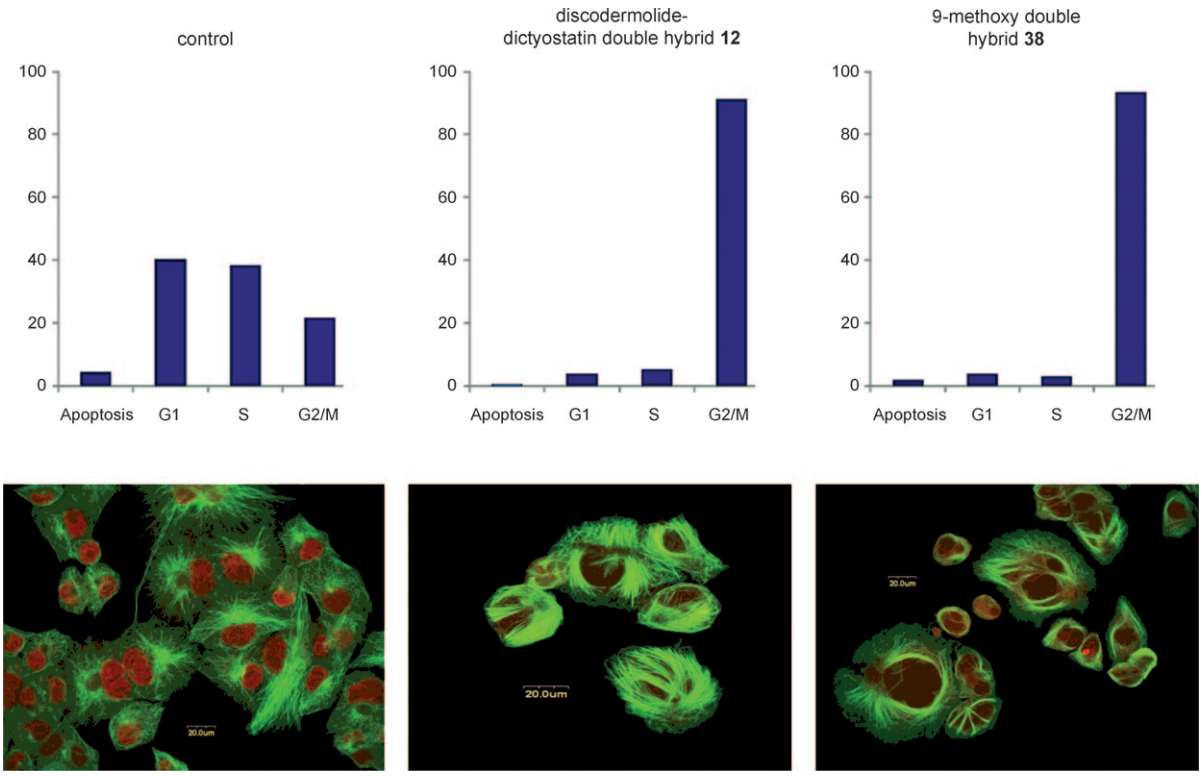

Figure 3. Graphs: Cell-cycle analysis by flow cytometry of PANC-1 cells incubated for 24 h with DMSO (control), 100 nM discodermolide/dictyostatin hybrid **12**, or 9-methoxy derivative **38**. Histograms represent samples of approximately 1×10^4 cells per test and are plotted as percentage (y axis) versus stage of cell cycle (x axis). Both compounds result in an accumulation of cells in the G2/M phase. Images: Immunofluorescence images of PANC-1 cells stained with *anti*-α-tubulin (green) and propidium iodide (red) and observed with confocal microscopy. Cells were exposed to DMSO (control, left-hand image), 100 nM **12** (middle image) or 100 nM **38** (right-hand image). Dense microtubule bundling can be seen around the nuclei on treatment with **12** and **38**, a characteristic feature of microtubule-stabilizing agents. DMSO = dimethyl sulfoxide.

Experimental Section

General: Full experimental details and characterization data for all hybrids and intermediates can be found in the Supporting Information.

Double hybrid 5: R_f = 0.39 (100% EtOAc); R_t = 28 min (10% IPA/hexane); $[\alpha]_{20}^{D}$ = +71.6 (c = 0.27 in $CHCl_3$); IR (thin film): $\tilde{\nu}_{max}$ = 3385, 2963, 2929, 2873, 1713, 1640, 1454, 1413, 1379 cm^{-1}; ^1H NMR (700 MHz, CD_3OD): δ = 6.62 (1H, dt, J = 17.0, 10.6 Hz; H25), 6.08 (1H, t, J = 10.9 Hz; H3), 5.98 (1H, t, J = 10.9 Hz; H24), 5.65 (1H, d, J = 11.8 Hz; H2), 5.57 (1H, dd, J = 9.0, 10.9 Hz; H11), 5.30 (1H, t, J = 10.1 Hz; H10), 5.19 (1H, brt, J = 9.0 Hz; H23), 5.16 (1H, d, J = 17.0 Hz; H26a), 5.08 (1H, d, J = 10.1 Hz; H26b), 4.88 (1H, brd, J = 4.9 Hz; H21), 4.83 (1H, d, J = 10.2 Hz; H15), 4.50 (1H, brd, J = 8.3 Hz; H9), 4.12 (1H, brdd, J = 3.9, 9.7 Hz; H7), 3.55 (1H, brs; H4), 3.37–3.32 (1H, m; H5), 3.07–3.02 (2H, m; H13, H22), 2.98 (1H, brs; H19), 2.56 (1H, quin., J = 7.7 Hz, H12), 2.40–2.35 (1H, m; H14), 2.32 (1H, brs; H17a), 2.11 (1H, brs; H18), 1.96–1.91 (1H, m; H20), 1.78 (1H, sex., J = 7.2 Hz; H6), 1.65 (3H, s; Me16), 1.53 (1H, d, J = 12.6 Hz; H17b), 1.36 (1H, ddd, J = 2.6, 11.4, 13.8 Hz; H8a), 1.24 (1H, dd, J = 2.9, 10.7 Hz; H8b), 1.05 (3H, d, J = 7.2 Hz; Me12), 0.97 (3H, d, J = 6.8 Hz; Me20), 0.95 (3H, d, J = 6.8 Hz; Me4), 0.93 (3H, d, J = 6.8 Hz; Me14), 0.91 (3H, d, J = 6.8 Hz; Me22), 0.84 (3H, d, J = 7.0 Hz; Me6), 0.64 ppm (3H, d, J = 6.3 Hz; Me18); ^{13}C NMR (175 MHz, CD_3OD): δ = 173.0 (C1), 167.6 (C16), 135.3 (C10), 134.5 (C23), 133.6 (C25), 131.4 (C24), 131.3 (C15), 131.0 (C11), 119.6 (C2), 118.4 (C26), 80.8 (C13), 78.6 (C5), 78.1 (C21), 77.0 (C19), 68.2 (C7), 65.1 (C9), 43.4 (C6), 38.6 (C17), 38.4 (C8), 38.3 (2C, C14, C20), 37.2 (C4), 35.8 (C12), 35.5 (C22), 32.8 (C18), 23.2 (Me16), 19.9 (Me12), 19.3 (Me22), 17.8 (Me14), 12.8 (Me4), 12.0 (Me6), 11.7 (Me18), 10.1 ppm (Me20); HRMS (ES+): m/z: calcd for $C_{34}H_{56}O_7Na$: 599.3918 $[M+Na]^+$, found: 599.3923.

Double hybrid 12: R_f = 0.48 (100% EtOAc); R_t = 15 min (10% IPA/hexane); $[\alpha]_{20}^{D}$ = −106.9 (c = 0.38 in $CHCl_3$); IR (neat): $\tilde{\nu}_{max}$ = 3406, 2965, 2931, 1687, 1638, 1453 cm^{-1}; ^1H NMR (500 MHz, C_6D_6): δ = 7.51 (1H, dd, J = 11.2, 15.6 Hz; H4), 6.64 (1H, ddd, J = 10.5, 10.6, 16.8 Hz; H25), 6.25 (1H, t, J = 11.6 Hz; H3), 6.02 (1H, t, J = 11.0 Hz; H24), 5.88 (1H, dd, J = 7.7, 15.5 Hz; H5), 5.63 (1H, d, J = 11.7 Hz; H2), 5.53–5.64 (2H, m; H10, H11), 5.40 (1H, t, J = 10.5 Hz; H23), 5.30 (1H, dd, J = 3.0, 8.6 Hz; H21), 5.12 (1H, d, J = 17.0 Hz; H26a), 5.00 (2H, t, J = 12.0 Hz; H15, H26b), 4.66 (1H, dq, J = 4.0, 7.8 Hz; H9), 4.01 (1H, d, J = 10.6 Hz; H7), 3.27 (1H, dd, J = 2.4, 8.6 Hz; H19), 3.04–3.13 (2H, m; H13, H22), 2.65–2.78 (2H, m; H12, H14), 2.30–2.38 (2H, m; H6, H18), 2.00–2.18 (3H, m; H17a, H17b, H20), 1.79 (3H, s; Me16), 1.67 (1H, ddd, J = 3.8, 10.4, 14.3 Hz; H8a), 1.46 (1H, ddd, J = 2.3, 7.8, 14.1 Hz; H8b), 1.25 (3H, d, J = 6.7 Hz; Me20), 1.17 (3H, d, J = 6.8 Hz; Me6), 1.07 (3H, d, J = 6.9 Hz; Me12), 1.05 (3H, d, J = 7.0 Hz; Me14), 0.96 (3H, d, J = 6.6 Hz; Me18), 0.87 ppm (3H, d, J = 6.6 Hz; Me22); ^{13}C NMR (125 MHz, C_6D_6): δ = 166.2 (C1), 144.9 (C5), 143.2 (C3), 134.8 (C23), 134.5 (C10), 134.0 (C11), 132.7 (C25), 132.6 (C16), 130.4 (C24), 128.6 (C15), 127.9 (C4), 118.1 (C2), 118.0 (C26), 79.5 (C13), 76.8 (C21), 74.8 (C19), 71.1 (C7), 66.0 (C9), 43.3 (C6), 40.8 (C8), 37.8 (C14), 37.6 (C17), 37.2 (C20), 35.4 (C22), 35.2 (C12), 31.8 (C18), 23.2 (Me16), 20.0 (Me12), 19.3 (Me14), 17.2 (Me22), 15.6 (Me6), 12.7 (Me18), 10.8 ppm (Me20); HRMS (ESI+): m/z: calcd for $C_{33}H_{53}O_6$: 545.3842 $[M+H]^+$, found: 545.3864.

Double hybrid 23: R_f = 0.37 (100% EtOAc); R_t = 12 min (10% IPA/hexane); $[\alpha]_{20}^{D}$ = −64.6 (c = 0.3 in $CHCl_3$); IR (neat): $\tilde{\nu}_{max}$ = 3395, 2963, 2928, 1683, 1638, 1454, 1407, 1378 cm^{-1}; ^1H NMR (500 MHz, C_6D_6): δ = 7.43 (1H, dd, J = 11.2 Hz; H4), 6.56 (1H, dt, J = 10.9, 16.9 Hz; H25), 6.21 (1H, t, J = 11.5 Hz; H3), 6.10 (1H, t, J = 10.7 Hz; H24), 5.74 (1H, dd, J = 8.8, 15.4 Hz; H5), 5.67 (1H, d, J = 11.7 Hz; H2), 5.60 (1H, t, J = 10.7 Hz; H23), 5.49 (1H, t, J = 6.2 Hz; H21), 5.19 (1H, d, J = 16.8 Hz; H26b), 5.04

(1H, d, J=10.4 Hz; H26a), 4.92 (1H, d, J=10.6 Hz; H15), 3.65–3.71 (2H, m; H7, H9), 3.35 (1H, t, J=5.4 Hz; H19), 3.14 (1H, ddd, J=6.7, 13.4, 18.0 Hz; H22), 3.04 (1H, dd, J=1.7, 7.7 Hz; H13), 2.62 (1H, ddd, J=6.6, 13.7, 17.2 Hz; H14), 2.35–2.43 (1H, m; H6), 2.08–2.15 (1H, m; H20), 2.05 (2H, d, J=6.8 Hz; H17a, H17b), 1.93 (12H, dt, J=7.0, 13.5 Hz; H18), 1.87 (1H, brs; H10a), 1.71 (2H, t, J=7.2 Hz; H10b, H11a), 1.65 (3H, s; Me16), 1.49–1.55 (2H, m; H11b, H12), 1.40–1.45 (1H, m; H8a), 1.17–1.22 (1H, m; H8b), 1.14 (3H, d, J=6.8 Hz; Me20), 1.01 (3H, obsd, J=6.3 Hz; Me14), 1.00 (3H, obsd, J=6.9 Hz; Me6), 0.98 (3H, obsd, J=7.1 Hz; Me22), 0.93 (3H, obsd, J=6.8 Hz; Me12), 0.92 ppm (3H, obsd, J=6.4 Hz; Me18); ^{13}C NMR (500 MHz, C_6D_6): δ= 166.5 (C1), 145.0 (C5), 142.2 (C3), 34.4 (C23), 133.4 (C16), 132.6 (C25), 130.2 (C24), 129.9 (C15), 129.3 (C4), 118.7 (C2), 118.2 (C26), 81.0 (C13), 78.1 (C21), 75.3 (C19), 72.5 (C7), 70.0 (C9), 44.0 (C6), 40.7 (C12), 37.9 (C20), 37.1 (C14), 36.3 (C8), 35.8 (C17), 34.8 (C22), 32.9 (C18), 32.0 (C10), 25.3 (C11), 23.0 (Me16), 18.8 (Me14), 17.7 (Me22), 17.2 (Me16), 14.4 (Me18), 14.0 (Me12), 10.4 ppm (Me20); HRMS (ESI+) m/z: calcd for $C_{33}H_{55}O_6$: 547.3999 $[M+H]^+$, found: 547.4013.

Acetonide 18: R_f=0.66 (40% EtOAc); R_t=16 min (25% EtOAc/hexane); $[\alpha]_{20}^{D}$=−20.0 (c=0.06 in $CHCl_3$); IR (neat): $\tilde{\nu}_{max}$=3395, 2923, 2853, 1713, 1641, 1456 cm^{-1}; ^{1}H NMR (500 MHz, C_6D_6): δ=7.60 (1H, dd, J=11.0, 15.0 Hz; H4), 6.67 (1H, ddd, J=9.5, 10.6, 16.5 Hz; H25), 6.24 (1H, t, J=11.0 Hz; H3), 5.99 (1H, t, J=10.9 Hz; H24), 5.77 (1H, dd, J= 7.0, 15.9 Hz; H5), 5.53–5.68 (3H, m; H2, H10, H11), 5.31 (1H, t, J= 10.9 Hz; H23), 5.23 (1H, dd, J=2.3, 9.1 Hz; H21), 5.10 (1H, d, J= 16.8 Hz; H26a), 5.03 (1H, d, J=10.5 Hz; H26b), 4.95 (1H, d, J=10.5 Hz; H15), 4.58 (1H, dq, J=6.4, 9.9 Hz; H9), 3.87 (1H, ddd, J=3.2, 6.4, 9.0 Hz; H7), 3.08 (1H, d, J=9.5 Hz; H19), 3.03 (1H, dq, J=6.4, 14.9 Hz; H22), 2.95 (1H, dd, J=3.7, 7.8 Hz; H13), 2.66–2.74 (1H, m; H12), 2.62 (1H, q, J=8.2 Hz; H14), 2.50–2.56 (1H, m; H6), 2.43–2.50 (1H, m; H18), 2.28 (1H, t, J=12.3 Hz; H17a), 1.98 (1H, ddd, J=2.8, 7.3, 9.6 Hz; H20), 1.89–1.95 (1H, m; H17b), 1.86 (3H, s; Me16), 1.79 (1H, ddd, J=5.9, 9.1, 14.9 Hz; H8a), 1.41 (3H, s; C(CH$_3$)$_2$), 1.38 (3H, s; C(CH$_3$)$_2$), 1.28–1.35 (1H, m; H8b), 1.24 (3H, d, J=6.8 Hz; Me6), 1.15 (3H, d, J=7.2 Hz; Me20), 1.06 (3H, d, J=6.9 Hz; Me12), 1.03 (3H, d, J=6.9 Hz; Me14), 0.95 (3H, d, J=6.8 Hz; Me18), 0.80 ppm (3H, d, J=7.3 Hz; Me22); ^{13}C NMR (125 MHz, C_6D_6): δ=165.8, 144.3, 143.8, 135.0, 134.6, 132.9, 132.8, 131.9, 130.3, 127.8, 117.8, 117.7, 100.6, 79.9, 76.0, 75.2, 68.2, 67.9, 63.9, 40.6, 37.6, 37.5, 36.2, 35.1, 34.2, 31.3, 25.9, 25.2, 24.7, 23.3, 19.5, 19.3, 17.0, 11.6, 10.4 ppm; HRMS (ESI+): m/z: calcd for $C_{36}H_{56}O_6Na$: 607.3975 $[M+Na]^+$, found: 607.3994.

Triple hybrid 31: R_f=0.63 (80% EtOAc/petroleum ether); R_t=15.0 min (8% IPA/hexane); $[\alpha]_{20}^{D}$==+23.3 (c=0.03 in $CHCl_3$); IR (neat): $\tilde{\nu}_{max}$= 3348, 2923, 2853, 1711, 1647, 1520, 1461 cm^{-1}; ^{1}H NMR (500 MHz, [D$_7$]DMF): δ=8.83 (1H, d, J=8.9 Hz; NH), 8.00 (2H, d, J=8.3 Hz; Ar), 7.60 (2H, d, J=7.8 Hz; Ar), 7.57 (2H, d, J=7.6 Hz; Ar), 7.50 (2H, t, J= 7.7 Hz; Ar), 7.37–7.43 (1H, m; Ar), 7.32 (1H, t, J=7.5 Hz; Ar), 7.23 (1H, t, J=12.3 Hz; H4), 6.70–6.80 (2H, m; H3, H25), 6.24 (1H, dd, J= 5.8, 15.6 Hz; H5), 6.05–6.13 (1H, m; H24), 5.77 (1H, dd, J=2.9, 9.0 Hz; H11), 5.65–5.72 (2H, m; H2, H3'), 5.36 (1H, d, J=9.0 Hz; H23), 5.31–5.35 (1H, m; H7), 5.28 (2H, d, J=16.3 Hz; H10, H26a), 5.18 (1H, d, J= 10.2 Hz; H26b), 5.07 (1H, t, J=5.8 Hz; H21), 4.98 (1H, d, J=10.2 Hz; H15), 4.70 (1H, d, J=2.8 Hz; C13-O*H*), 4.62 (1H, d, J=4.1 Hz; C19-O*H*), 4.55–4.61 (2H, m; H9, H2'), 3.18–3.26 (1H, m; H22), 3.08–3.16 (2H, t, J=10.2 Hz; H13, H19), 2.54–2.61 (1H, m; H6), 2.41–2.49 (1H, m; H12), 2.24–2.32 (1H, m; H14), 2.02–2.08 (1H, m; H18), 1.99 (1H, q, J= 6.1 Hz; H20), 1.74 (3H, s; Me16), 1.55 (2H, q, J=11.2 Hz; H8a, H17a), 1.37–1.43 (1H, m; H8b), 1.33–1.37 (1H, m; H17b), 1.15 (3H, d, J= 7.1 Hz; Me12), 1.06 (3H, d, J=6.9 Hz; Me20), 1.05 (3H, d, J=6.9 Hz; Me6), 0.99 (6H, t, J=6.3 Hz; Me14, Me22), 0.74 ppm (3H, d, J=6.3 Hz; Me18); HRMS (ES+): m/z: calcd for $C_{49}H_{66}NO_9$: 812.4738 $[M+H]^+$, found: 812.4736.

Double hybrid 32: R_f=0.56 (70% EtOAc/petroleum ether); R_t=13.5 min (7% IPA/hexane); $[\alpha]_{20}^{D}$=−20.0 (c=0.02 in $CHCl_3$); IR (neat): $\tilde{\nu}_{max}$= 3450, 2963, 2918, 1696, 1498, 1457 cm^{-1}; ^{1}H NMR (500 MHz, C_6D_6): δ= 7.68 (1H, t, J=13.5 Hz; H4), 7.38 (2H, d, J=7.4 Hz; Ar), 7.11 (2H, obsd, J=7.7 Hz; Ar), 7.05 (1H, t, J=7.4 Hz; Ar), 6.66 (1H, ddd, J= 10.7, 10.8, 16.8 Hz; H25), 6.13 (1H, t, J=11.0 Hz; H3), 5.98 (1H, t, J= 11.0 Hz; H24), 5.66–5.81 (2H, m, H7; H11), 5.63 (1H, dd, J=6.1, 16.2 Hz; H5), 5.58 (1H, d, J=11.3 Hz; H2), 5.45 (1H, d, J=10.1 Hz; NH), 5.34 (1H, d, J=10.1 Hz; H3'), 5.26 (1H, t, J=10.4 Hz; H23), 5.20 (1H, dd, J=2.5, 8.9 Hz; H21), 5.11 (1H, d, J=16.8 Hz; H26a), 5.03 (2H, d, J=10.6 Hz; H10, H26b), 4.89 (1H, d, J=10.1 Hz; H15), 4.41 (1H, d, J=5.5 Hz; H2'), 4.33 (1H, d, J=5.1 Hz; H9), 3.11–3.18 (1H, m; H6), 3.05 (2H, d, J=5.5 Hz; H13, C2'-O*H*), 2.99 (2H, t, J=9.2 Hz; H19, H22), 2.71 (1H, t, J=2.7 Hz; H12), 2.61 (1H, q, J=6.4 Hz; H14), 2.45–2.56 (2H, m; H17a, H18), 1.94 (3H, s; Me16), 1.89–1.93 (1H, obsm; H20), 1.81 (1H, dt, J=2.8, 13.1 Hz; H8a), 1.70 (1H, d, J=11.1 Hz; H8a), 1.65 (1H, dt, J=2.8, 13.0 Hz; H17b), 1.34 (3H, d, J=7.1 Hz; Me12), 1.28 (9H, s; C(CH$_3$)$_3$), 1.10 (3H, d, J=7.1 Hz; Me6), 1.08 (3H, d, J=6.9 Hz; Me20), 1.06 (3H, d, J=6.7 Hz; Me14), 0.88 (3H, d, J=6.5 Hz; Me18), 0.77 ppm (3H, d, J=6.7 Hz; Me22); ^{13}C NMR (125 MHz, CD_2Cl_2): δ= 173.2 (C1'), 166.3 (C1), 156.3 (*t*BuO*C*(O)NHR), 143.9 (C3), 142.9 (C5), 140.4 (Ar), 134.8 (C10, C23), 133.8 (C16), 132.9 (C25), 130.5 (C24), 129.7 (C11), 129.4 (C15), 129.3 (Ar), 128.5 (Ar), 128.0 (C4), 127.4 (2C, Ar), 118.15 (C2), 118.10 (C26), 81.1 (*C*Me$_3$), 80.1 (C13), 76.7 (C21), 76.5 (C19), 75.7 (C7), 73.5 (C2'), 63.9 (C9), 56.8 (C3'), 38.7 (C6), 37.8 (C17), 37.51 (C20), 37.47 (C14), 35.3 (C12), 35.1 (C8), 35.0 (C6), 31.5 (C18), 28.6 (3C, C*Me*$_3$), 23.5 (Me16), 19.3 (Me14), 19.0 (Me12), 17.3 (Me22), 12.3 (Me6), 11.5 (Me18), 10.0 ppm (Me20); HRMS (ES+): m/z: calcd for $C_{47}H_{69}NO_{10}Na$: 830.4819 $[M+Na]^+$, found: 830.4858.

Double hybrid 33: R_f=0.63 (80% EtOAc/petroleum ether); R_t=9.1 min (8% IPA/hexane); $[\alpha]_{20}^{D}$=+6.6 (c=0.03 in $CHCl_3$); IR (neat): $\tilde{\nu}_{max}$=3363, 2922, 2853, 1715, 1655, 1517, 1457 cm^{-1}; ^{1}H NMR (500 MHz, [D$_7$]DMF): δ=8.71 (1H, d, J=9.1 Hz; NH), 7.99 (2H, d, J=7.3 Hz; Ar), 7.55–7.61 (3H, m; Ar), 7.52 (2H, t, J=7.8 Hz; Ar), 7.41 (2H, t, J=7.5 Hz; Ar), 7.33 (1H, t, J=7.3 Hz; Ar), 7.20 (1H, t, J=13.1 Hz; H4), 6.72–6.81 (2H, m; H3, H25), 6.24 (1H, dd, J=6.1, 15.8 Hz; H5), 6.09 (1H, t, J=10.9 Hz; H24), 6.05 (1H, d, J=9.5 Hz; C2'-O*H*), 5.79 (1H, t, J=9.5 Hz; H11), 5.73 (1H, t, J=9.2 Hz; H9), 5.68–5.71 (1H, obsm; H3'), 5.67 (1H, obsd, J=10.4 Hz; H2), 5.38 (1H, t, J=10.7 Hz; H23), 5.30 (1H, obsd, J= 15.8 Hz; H26a), 5.29 (1H, obst, J=9.6 Hz; H10), 5.20 (1H, d, J= 10.4 Hz; H26b), 5.07 (1H, t, J=5.8 Hz; H21), 4.91 (1H, d, J=10.2 Hz; H15), 4.81 (1H, d, J=5.6 Hz; C13-O*H*), 4.71 (1H, d, J=5.3 Hz; C19-O*H*), 4.63 (1H, t, J=4.4 Hz; H2'), 4.53 (1H, d, J=5.3 Hz; C7-O*H*), 3.21–3.28 (1H, m; H22), 3.13–3.18 (1H, m; H19), 3.10 (1H, dd, J=6.1, 9.5 Hz; H13), 2.57 (1H, q, J=6.1 Hz; H6), 2.50 (1H, t, J=7.5 Hz; H12), 2.36 (1H, q, J=8.5 Hz; H14), 2.00 (2H, q, J=6.1 Hz; H18, H20), 1.69 (3H, s; Me16), 1.57 (1H, d, J=12.1 Hz; H17a), 1.48 (1H, t, J=11.2 Hz; H8a), 1.41 (1H, dt, J=3.2, 10.4 Hz; H8b), 1.25–1.31 (1H, m; H17b), 1.13 (3H, d, J=7.1 Hz; Me12), 1.05 (6H, t, J=6.3 Hz; Me6, Me20), 0.99 (3H, d, J=6.8 Hz; Me22), 0.96 (3H, d, J=6.6 Hz; Me14), 0.74 ppm (3H, d, J= 6.7 Hz; Me18); ^{13}C NMR (125 MHz, [D$_7$]DMF): δ=172.0, 167.8, 166.8, 145.9, 144.0, 140.9, 135.1, 134.1, 133.7, 133.5, 133.1, 132.3, 130.7, 130.6, 129.5, 129.1 (2C), 129.0 (2C), 128.2 (2C), 128.1 (2C), 128.0, 127.3, 118.2, 117.8, 79.1, 78.8, 75.4, 75.0, 70.2, 68.1, 56.9, 43.0, 38.0, 37.8, 37.3, 36.6, 34.6, 32.7, 23.2 (2C), 23.1, 19.4, 18.7, 18.0, 14.3, 13.6, 12.3, 10.0 ppm; HRMS (ES+): m/z: calcd for $C_{49}H_{66}NO_9$: 812.4738 $[M+H]^+$, found: 812.4734.

Double hybrid 34: R_f=0.56 (70% EtOAc/petroleum ether); R_t=9.5 min (7% IPA/hexane); $[\alpha]_{20}^{D}$=+6.0 (c=0.03 in $CHCl_3$); IR (neat): $\tilde{\nu}_{max}$=3433, 2963, 2920, 1694, 1498, 1456 cm^{-1}; ^{1}H NMR (500 MHz, CD_2Cl_2): δ=7.36–7.42 (4H, m; Ar), 7.29–7.34 (1H, m; Ar), 7.28 (1H, dd, J=4.4, 15.4 Hz; H4), 6.64 (1H, ddd, J=10.9, 11.0, 16.9 Hz; H25), 6.54 (1H, t, J=11.0 Hz; H3), 6.08 (1H, dd, J=7.0, 15.6 Hz; H5), 5.99 (1H, t, J=11.0 Hz; H24), 5.65 (1H, obsdd, J=8.6, 11.0 Hz; H11), 5.58–5.63 (1H, m; H9), 5.50 (2H, d, J=11.2 Hz; H2, NH), 5.27–5.35 (2H, m; H10, H23), 5.15–5.20 (2H, m; H26a, H3'>), 5.09 (1H, d, J=10.0 Hz; H26b), 4.99 (2H, dd, J= 2.7, 9.0 Hz; H15, H21), 4.44 (1H, d, J=4.5 Hz; H2'), 4.00 (1H, d, J= 9.8 Hz; H7), 3.68 (1H, brs; OH), 3.24 (1H, dd, J=3.4, 8.5 Hz; H13), 3.13 (1H, d, J=4.6 Hz; C2'-O*H*), 3.06 (2H, d, J=7.6 Hz; H19, H22), 2.62–2.68 (1H, m; H12), 2.49–2.58 (2H, m; H6, H14), 2.05–2.13 (2H, m; H17a, H18), 1.95 (1H, ddd, J=2.5, 3.0, 6.7 Hz; H20), 1.75 (1H, d, J= 7.8 Hz; H17b), 1.65 (3H, s; Me16), 1.47–1.60 (2H, m; H8a, H8b), 1.42 (9H, s; C(CH$_3$)$_3$), 1.16 (6H, t, J=6.9 Hz; Me6, Me12), 1.12 (3H, d, J= 6.7 Hz; Me20), 1.01 (3H, d, J=6.7 Hz; Me22), 0.99 (3H, d, J=6.8 Hz; Me14), 0.74 ppm (3H, d; Me18); ^{13}C NMR (125 MHz, CD_2Cl_2): δ=173.0

(C1'), 166.4 (C1), 156.3 (*t*BuO*C*(O)NHR), 145.7 (C5), 143.8 (C3), 139.9 (Ar), 135.1 (C23), 134.4 (C16), 133.2 (C11), 132.9 (C25), 130.3 (C24), 129.5 (C10), 129.2 (2C, Ar), 129.0 (C15), 128.3 (Ar), 127.9 (C4), 127.3 (2C, Ar), 118.0 (C26), 117.7 (C2), 81.1 (*C*Me$_3$), 79.9 (C13), 76.7 (C21), 75.7 (C19), 73.6 (C2'), 72.3 (C9), 69.2 (C7), 56.6 (C3'), 43.7 (C6), 37.7 (C20), 37.4 (3C, C8, C14, C17), 35.5 (C12), 35.1 (C22), 31.6 (C18), 28.6 (C*Me*$_3$), 23.3 (Me16), 19.2 (Me14), 17.7 (Me12), 17.4 (Me22), 13.8 (Me6), 12.0 (Me18), 10.5 ppm (Me20); HRMS (ES$^+$): *m*/*z*: calcd for $C_{47}H_{70}NO_{10}$: 808.5000 $[M+H]^+$, found: 808.5028.

Double hybrid 38: R_f = 0.54 (70 % EtOAc/petroleum ether); R_t = 20.0 min (4.5 % IPA/hexane); $[\alpha]_{20}^{D} = -109.4$ (*c* = 0.17 in $CHCl_3$); IR (neat): $\tilde{\nu}_{max}$ = 3456, 2961, 2928, 1699, 1638, 1457 cm^{-1}; ^{1}H NMR (500 MHz, CD_2Cl_2): δ = 7.14 (1H, dd, *J* = 11.3, 15.8 Hz; H4), 6.60 (1H, dddd, *J* = 0.9, 10.6, 11.0, 16.9 Hz; H25), 6.49 (1H, dt, *J* = 0.6, 11.4 Hz; H3), 5.98 (1H, obs dd, *J* = 6.4, 8.9 Hz; H5), 5.94 (1H, obs t, *J* = 4.1 Hz; H24), 5.57 (1H, t, *J* = 10.0 Hz; H11), 5.45 (1H, obs d, *J* = 11.6 Hz; H2), 5.45 (1H, obs dd, *J* = 9.4, 11.2 Hz; H10), 5.29 (1H, t, *J* = 10.4 Hz; H23), 5.15 (1H, dt, *J* = 2.0, 16.7 Hz; H26a), 5.06 (2H, t, *J* = 12.4 Hz; H15, H26b), 5.00 (1H, dd, *J* = 3.0, 8.8 Hz; H21), 4.22 (1H, qu, *J* = 4.5 Hz; H9), 3.84 (1H, ddd, *J* = 2.3, 4.5, 10.3 Hz; H7), 3.31 (1H, t, *J* = 6.3 Hz; H13), 3.24 (3H, s; OMe), 3.10 (1H, dd, *J* = 2.8, 8.9 Hz; H19), 3.05 (1H, q, *J* = 7.4 Hz; H22), 2.75–2.83 (2H, m; H12, H14), 2.49–2.63 (1H, br s; OH), 2.22–2.28 (1H, m; H6), 2.11 (1H, dd, *J* = 8.8, 13.5 Hz; H17a), 1.89–1.99 (2H, m; H18, H20), 1.83 (1H, dd, *J* = 7.2, 13.2 H; H17b), 1.52–1.57 (2H, m; H8a, H8b), 1.51 (3H, s; Me16), 1.14 (3H, d, *J* = 6.8 Hz; Me20), 1.11 (3H, d, *J* = 6.8 Hz; Me6), 1.08 (3H, d, *J* = 6.8 Hz; Me12), 1.01 (3H, d, *J* = 6.7 Hz; Me22), 0.97 (3H, d, *J* = 6.9 Hz; Me14), 0.81 ppm (3H, d, *J* = 6.5 Hz; Me18); ^{13}C NMR (125 MHz, CD_2Cl_2): δ = 166.7 (C1), 145.4 (C5), 142.6 (C3), 135.25 (C16),135.19 (2C, C11, C23), 132.8 (C25), 132.1 (C10), 130.2 (C24), 128.9 (C4), 127.9 (C15), 118.4 (C2), 118.0 (C26), 79.4 (C13), 77.2 (C21), 75.6 (C9), 73.7 (C19), 71.9 (C7), 56.6 (OMe), 45.0 (C6), 40.6 (C8), 37.82 (C20), 37.76 (C14), 36.9 (C17), 35.5 (C22), 35.2 (C12), 31.7 (C18), 23.1 (Me16), 19.5 (Me12), 19.1 (Me14), 17.5 (Me22), 16.3 (Me6), 13.1 (Me8), 11.2 ppm (Me20); HRMS (ES+): *m*/*z*: calcd for $C_{34}H_{55}O_6$: 559.3999 $[M+H]^+$, found: 599.3998.

Double hybrid 44: R_f = 0.37 (70 % EtOAc/petroleum ether); R_t = 34.9 min (6 % IPA/hexane); $[\alpha]_{20}^{D} = -24.4$ (*c* = 0.09 in $CHCl_3$); IR (neat): $\tilde{\nu}_{max}$ = 3402, 2928, 1672, 1638, 1451 cm^{-1}; ^{1}H NMR (500 MHz, CD_2Cl_2): δ = 7.26 (1H, dd, *J* = 11.3, 15.8 Hz; H4), 6.64 (1H, dddd, *J* = 0.9, 10.7, 10.8, 16.9 Hz; H25), 6.52 (1H, t, *J* = 11.4 Hz; H3), 6.02 (1H, dd, *J* = 6.6, 9.2 Hz; H5), 5.99 (1H, t, *J* = 10.6 Hz; H24), 5.58 (1H, dd, *J* = 9.0, 11.4 Hz; H11), 5.49 (1H, d, *J* = 11.4 Hz; H2), 5.37 (1H, dd, *J* = 8.4, 11.3 Hz; H10), 5.29 (1H, obs t, *J* = 10.6 Hz; H23), 5.18 (1H, dd, *J* = 1.9, 16.8 Hz; H26a), 5.10 (1H, d, *J* = 10.2 Hz; H26b), 4.98 (1H, dd, *J* = 3.5, 8.4 Hz; H21), 4.95 (1H, d, *J* = 9.9 Hz; H15), 4.45 (1H, t, *J* = 8.0 Hz; H9), 3.52 (1H, ddd, *J* = 3.5, 6.4, 6.9 Hz; H7), 3.39 (3H, s; OMe), 3.21 (1H, dd, *J* = 3.3, 8.4 Hz; H13), 3.02–3.09 (2H, m; H19, H22), 2.77 (1H, q, *J* = 6.4 Hz; H6), 2.63 (1H, tt, *J* = 1.7, 8.0 Hz; H12), 2.48 (1H, q, *J* = 9.5 Hz; H14), 1.99–2.09 (2H, m; H17a, H18), 1.94 (1H, ddd, *J* = 1.6, 3.6, 6.8 Hz; H20), 1.67–1.72 (1H, m; H17b), 1.64 (3H, s; Me16), 1.37–1.43 (1H, m; H8a), 1.31–1.36 (1H, m; H8b), 1.08 (9H, d, *J* = 7.3 Hz; Me6, Me12, Me20), 0.99 (6H, t, *J* = 6.8 Hz; Me14, Me22), 0.72 ppm (3H, d, *J* = 6.1 Hz; Me18); ^{13}C NMR (125 MHz, CD_2Cl_2): δ = 166.5 (C1), 145.6 (C5), 144.0 (C3), 134.8 (C23), 134.5 (C16), 134.3 (C10), 132.9 (C25), 131.8 (C11), 130.4 (C24), 128.9 (C15), 127.9 (C4), 118.1 (C26), 117.4 (C2), 80.3 (C7), 80.1 (C13), 76.9 (C21), 75.7 (C19), 65.6 (C9), 58.3 (OMe), 39.1 (C6), 38.2 (C8), 37.59 (C14), 37.55 (C20), 37.3 (C17), 35.4 (C12), 35.1 (C19), 31.7 (C18), 23.2 (Me16), 19.6 (Me22), 19.3 (Me14), 17.5 (Me20), 13.5 (Me6), 12.2 (Me18), 10.3 ppm (Me20); HRMS (ES+): *m*/*z*: calcd for $C_{34}H_{55}O_6$: 559.3999 $[M+H]^+$, found: 559.4005.

Double hybrid 36: R_f = 0.50 (50 % EtOAc); R_t = 32 min (2.5 % IPA/hexane); $[\alpha]_{20}^{D} = -5.0$ (*c* = 0.10 in $CHCl_3$); IR (neat): $\tilde{\nu}_{max}$ = 3435, 2962, 2930, 1713, 1639, 1599 cm^{-1}; ^{1}H NMR (500 MHz, CD_2Cl_2): δ = 7.23 (1H, dd, *J* = 10.9, 15.2 Hz; H4), 6.64 (1H, dddd, *J* = 1.0, 10.7, 10.8, 16.8 Hz; H25), 6.52 (1H, t, *J* = 11.3 Hz; H3), 6.02 (1H, dd, *J* = 6.6, 9.1 Hz; H5), 5.99 (1H, t, *J* = 10.7 Hz; H24), 5.69 (1H, t, *J* = 8.4, 11.2 Hz; H11), 5.48 (1H, d, *J* = 11.3 Hz; H2), 5.29 (1H, t, *J* = 10.3 Hz; H23), 5.16–5.21 (1H, m; H10), 5.10 (1H, d, *J* = 10.3 Hz; H26a), 4.98 (1H, dd, *J* = 3.5, 8.4 Hz; H21), 4.94 (1H, d, *J* = 10.1 Hz; H15), 3.96 (1H, dt, *J* = 3.9, 9.6 Hz; H9), 3.50 (1H, dt, *J* = 3.4, 10.4 Hz; H7), 3.36 (3H, s; OMe), 3.21 (3H, s; OMe), 3.20–3.24 (1H, obs m; H13), 3.02–3.08 (2H, m; H19, H22), 2.78 (1H, q, *J* = 6.2 Hz; H6), 2.46–2.55 (2H, m; H12, H14), 2.11 (2H, d, *J* = 7.8 Hz; H17a, H17b), 1.94 (1H, ddd, *J* = 1.7, 3.8, 7.0 Hz; H20), 1.59–1.67 (1H, obs m; H18), 1.64 (3H, s; Me16), 1.19–1.29 (2H, m; H8a, H8b), 1.11 (3H, d, *J* = 7.1 Hz; Me12) 1.09 (3H, d, *J* = 6.9 Hz; Me20) 1.05 (3H, d, *J* = 6.9 Hz; Me6), 0.99 (3H, d, *J* = 6.6 Hz; Me22), 0.98 (3H, d, *J* = 6.6 Hz; Me14), 0.71 ppm (3H, d, *J* = 6.2 Hz; Me18); ^{13}C NMR (125 MHz, CD_2Cl_2): δ = 166.4 (C1), 145.7 (C5), 143.9 (C3), 134.8 (C23), 134.1 (C16), 133.5 (C10), 132.9 (C25), 132.5 (C11), 130.4 (C24), 129.0 (C15), 127.6 (C4), 118.0 (C26), 117.4 (C2), 80.2 (C13), 79.4 (C7), 76.4 (C21), 75.9 (C19), 74.1 (C9), 58.1 (OMe), 56.4 (OMe), 38.9 (C6), 37.53 (C18, C20), 37.48 (C17), 37.3 (C14), 36.2 (C8), 35.1 (C22), 34.9 (C12), 23.3 (Me16), 19.3 (Me14), 18.9 (Me12), 17.4 (Me22), 12.6 (Me6), 12.0 (Me18), 10.3 ppm (Me20); HRMS (ESI+): *m*/*z*: calcd for $C_{35}H_{56}O_6Na$: 595.3975 $[M+Na]^+$, found: 595.3990.

Triple hybrid 39: R_f = 0.41 (60 % EtOAc/petroleum ether); R_t = 15.5 min (6 % IPA/hexane); $[\alpha]_{20}^{D} = -56.9$ (*c* = 0.13 in $CHCl_3$); IR (neat): $\tilde{\nu}_{max}$ = 3415, 2962, 2926, 1713, 1654, 1603, 1518, 1485, 1454 cm^{-1}; ^{1}H NMR (500 MHz, CD_2Cl_2): δ = 7.79 (2H, d, *J* = 7.7 Hz; Ar), 7.54 (1H, t, *J* = 7.6 Hz; Ar), 7.43–7.49 (4H, m; Ar), 7.40 (2H, t, *J* = 7.6 Hz; Ar), 7.34 (1H, d, *J* = 7.6 Hz; Ar), 7.30 (1H, d, *J* = 8.8 Hz; NH), 7.19 (1H, dd, *J* = 11.3, 15.6 Hz; H4), 6.61 (1H, ddd, *J* = 10.5, 10.8, 16.7 Hz; H25), 6.50 (1H, t, *J* = 11.6 Hz; H3), 5.97 (1H, t, *J* = 11.0 Hz; H24), 5.87 (1H, dd, *J* = 8.2, 15.8 Hz; H5), 5.70 (1H, dd, *J* = 1.5, 8.8 Hz; H3'), 5.52 (1H, obs t, *J* = 9.3 Hz; H11), 5.51 (1H, obs d, *J* = 11.8 Hz; H2), 5.34–5.38 (1H, m; H7), 5.28 (1H, t, *J* = 10.1 Hz; H23), 5.18 (1H, d, *J* = 7.4 Hz; H15), 5.15 (1H, obs t, *J* = 9.6 Hz; H10), 5.13 (1H, d, *J* = 14.5 Hz; H26a), 5.06 (1H, d, *J* = 10.2 Hz; H26b), 4.97 (1H, dd, *J* = 2.6, 9.1 Hz; H21), 4.64 (1H, s; H2'), 3.79 (1H, dd, *J* = 7.8, 14.7 Hz; H9), 3.47 (1H, d, *J* = 2.0 Hz; C2'-O*H*), 3.21 (1H, t, *J* = 4.8 Hz; H13), 3.02–3.08 (2H, m; H19, H22), 2.95 (3H, s; OMe), 2.63 (1H, dt, *J* = 2.8, 7.1 Hz; H6), 2.48–2.58 (2H, m; H12, H14), 1.98–2.05 (2H, m; H17a, H18), 1.95 (1H, ddd, *J* = 2.5, 6.8, 9.0 Hz; H20), 1.86–1.91 (1H, m; H17b), 1.60 (2H, t, *J* = 7.1 Hz; H8a, H8b), 1.57 (3H, d, *J* = 1.0 Hz; Me16), 1.14 (3H, d, *J* = 6.8 Hz; Me20), 1.00 (6H, d, *J* = 6.8 Hz; Me6, Me22), 0.95 (6H, t, *J* = 7.2 Hz; Me12, Me14), 0.78 ppm (3H, d, *J* = 6.5 Hz; Me18); ^{13}C NMR (125 MHz, CD_2Cl_2): δ = 172.3 (Ph*C*(O)NHR), 167.3 (C1'), 166.5 (C1), 142.9 (C3), 142.7 (C5), 139.9 (Ar), 136.3 (C11), 135.0 (C23), 134.0 (Ar), 132.8 (C25), 132.7 (C16), 132.6 (Ar), 131.8 (C10), 130.7 (C15), 130.3 (C24), 129.4 (C4), 129.2 (3C, Ar), 128.5 (Ar), 127.7 (2C, Ar), 127.3 (2C, Ar), 118.8 (C2), 118.0 (C26), 79.3 (C13), 76.9 (C21), 76.1 (C7), 74.3 (C2'), 74.2 (C19), 73.0 (C9), 56.2 (OMe), 55.3 (C3'), 41.5 (C6), 37.6 (C20), 37.3 (C8), 37.2 (C12), 37.1 (C17), 35.5 (C14), 35.4 (C22), 31.5 (C18), 23.1 (Me16), 18.2 (Me14), 17.4 (Me12), 17.3 (Me22), 15.2 (Me6), 12.7 (Me18) 11.1 ppm (Me20); HRMS (ES$^+$): *m*/*z*: calcd for $C_{50}H_{68}NO_9$: 826.4894 $[M+H]^+$, found: 826.4908.

Triple hybrid 40: R_f = 0.54 (60 % EtOAc/petroleum ether); R_t = 15.5 min (6 % IPA/hexane); $[\alpha]_{20}^{D} = -22.1$ (*c* = 0.14 in $CHCl_3$); IR (neat): $\tilde{\nu}_{max}$ = 3432, 2925, 2853, 1716, 1497, 1457 cm^{-1}; ^{1}H NMR (500 MHz, CD_2Cl_2): δ = 7.38 (4H, d, *J* = 4.4 Hz; Ar), 7.32 (1H, m; Ar), 7.27 (1H, dd, *J* = 11.1, 15.4 Hz; H4), 6.62 (1H, ddd, *J* = 10.4, 10.7, 16.8 Hz; H25), 6.52 (1H, t, *J* = 11.4 Hz; H3), 5.98 (1H, t, *J* = 10.9 Hz; H24), 5.92 (1H, dd, *J* = 7.3, 15.4 Hz; H5), 5.68 (1H, d, *J* = 10.2 Hz; NH), 5.65 (1H, t, *J* = 9.3 Hz; H11), 5.53 (1H, d, *J* = 11.6 Hz; H2), 5.28 (1H, t, *J* = 10.6 Hz; H23), 5.23–5.26 (1H, obs m; H7), 5.22 (1H, d, *J* = 9.4 Hz; H10), 5.17 (1H, dd, *J* = 2.0, 16.9 Hz; H26a), 5.11 (1H, d, *J* = 10.1 Hz; H15), 5.08–5.12 (1H, obs m; H3'), 5.07 (1H, d, *J* = 10.3 Hz; H26b), 4.97 (1H, dd, *J* = 3.0, 9.1 Hz; H21), 4.46 (1H, s; H2'), 3.93 (1H, dt, *J* = 5.3, 9.2 Hz; H9), 3.31 (1H, dd, *J* = 4.5, 6.1 Hz; H13), 3.23 (1H, s; C2'-O*H*), 3.17 (3H, s; OMe), 3.09 (1H, d, *J* = 9.0 Hz; H19), 3.05 (1H, dq, *J* = 7.3, 9.0 Hz; H22), 2.70–2.75 (1H, m; H6), 2.58–2.70 (2H, m; H12, H14), 2.13–2.22 (1H, br s; OH), 2.08 (1H, d, *J* = 6.9 Hz; H18), 1.88–2.02 (3H, m; H17a, H17b, H20), 1.63–1.71 (2H, m; H8a, H8b), 1.61 (3H, s; Me16), 1.38 (9H, s; C(CH$_3$)$_3$), 1.12 (3H, d, *J* = 6.7 Hz; Me20), 1.10 (3H, d, *J* = 6.9 Hz; Me12), 1.04 (3H, d, *J* = 7.0 Hz; Me6), 1.00 (3H, d, *J* = 6.8 Hz; Me22), 0.98 (3H, d, *J* = 6.8 Hz; Me14), 0.77 ppm (3H, d, *J* = 6.7 Hz; Me18); ^{13}C NMR (125 MHz, CD_2Cl_2): δ = 172.3 (C1'), 166.5 (C1), 155.8 (*t*BuO*C*(O)NHR), 143.1 (C3), 142.9 (C5), 140.7 (Ar), 135.8 (C11), 135.0 (C23), 133.6 (C16), 132.9 (C25), 131.9

(C10), 130.3 (C24), 129.7 (C15), 129.1 (Ar), 129.0 (Ar), 128.2 (C4), 127.1 (Ar), 118.7 (C2), 118.0 (C26), 80.4 (*C*Me$_3$), 79.8 (C13), 77.0 (C21), 75.8 (C19), 74.8 (C7), 74.7 (C2'), 74.0 (C9), 56.8 (C3'), 56.5 (OMe), 40.9 (C6), 37.6 (C20), 37.3 (C14), 36.5 (C8), 36.3 (C12), 36.2 (C17), 35.3 (C22), 31.5 (C18), 28.6 (3C, C*Me*$_3$), 23.3 (Me16), 18.8 (Me14), 18.2 (Me12), 17.4 (Me22), 14.5 (Me6), 12.4 (Me18), 10.7 ppm (Me20); HRMS (ES+): *m*/*z*: calcd for $C_{48}H_{72}NO_{10}$: 822.5156 $[M+H]^+$, found: 822.5158.

Triple hybrid 45: $R_f = 0.45$ (60% EtOAc/petroleum ether); $R_t = 102$ min (2% IPA/hexane); $[\alpha]_{20}^{D} = +46.0$ ($c = 0.05$ in $CHCl_3$); IR (neat): $\tilde{\nu}_{max} =$ 3427, 2959, 2934, 1711, 1651, 1518, 1486 cm^{-1}; ^{1}H NMR (500 MHz, CD_2Cl_2): $\delta = 7.81$ (2H, d, $J = 7.4$ Hz; Ar), 7.54 (1H, t, $J = 7.5$ Hz; Ar), 7.46 (4H, t, $J = 6.7$ Hz; Ar), 7.38 (2H, t, $J = 7.2$ Hz; Ar), 7.32 (1H, d, $J =$ 7.7 Hz; Ar), 7.25 (1H, dd, $J = 11.6$, 15.4 Hz; H4), 7.19 (1H, d, $J = 8.9$ Hz; NH), 6.65 (1H, ddd, $J = 10.3$, 10.7, 16.6 Hz; H25), 6.56 (1H, t, $J =$ 11.3 Hz; H3), 6.08 (1H, dd, $J = 6.2$, 15.7 Hz; H5), 6.00 (1H, t, $J = 11.0$ Hz; H24), 5.79 (1H, dt, $J = 3.9$, 10.4 Hz; H9), 5.70 (1H, d, $J = 8.6$ Hz; H3'), 5.67 (1H, obs dd, $J = 8.9$, 11.0 Hz; H11), 5.52 (1H, d, $J = 11.0$ Hz; H2), 5.27–5.31 (2H, m; H10, H23), 5.19 (1H, d, $J = 16.9$ Hz; H26a), 5.11 (1H, d, $J = 10.7$ Hz; H26b), 4.98 (1H, dd, $J = 3.6$, 8.2 Hz; H21), 4.96 (1H, d, $J = 10.5$ Hz; H15), 4.55 (1H, s; H2'), 3.36 (1H, d, $J = 2.4$ Hz; C2'-O*H*), 3.21 (1H, dd, $J = 3.0$, 8.8 Hz; H13), 3.16 (1H, ddd, $J = 1.8$, 4.2, 10.7 Hz; H7), 3.04–3.09 (2H, m; H19, H22), 2.98 (3H, s; OMe), 2.71 (1H, q, $J =$ 6.2 Hz; H6), 2.56 (1H, t, $J = 8.2$ Hz; H12), 2.47 (1H, q, $J = 8.8$ Hz; H14), 2.13 (2H, d, $J = 7.8$ Hz; H17a, H18), 1.94 (1H, dt, $J = 3.8$, 7.8 Hz; H20), 1.66 (3H, s; Me16), 1.56–1.63 (2H, m; H8a, H17b), 1.37 (1H, ddd, $J =$ 3.6, 11.1, 14.5 Hz; H8b), 1.10 (3H, d, $J = 7.2$ Hz; Me12), 1.09 (3H, d, $J =$ 7.0 Hz; Me20), 1.00 (3H, d, $J = 6.8$ Hz; Me22), 0.97 (3H, d, $J = 6.6$ Hz; Me14), 0.94 (3H, d, $J = 6.8$ Hz; Me6), 0.70 ppm (3H, d, $J = 5.6$ Hz; Me18); ^{13}C NMR (125 MHz, CD_2Cl_2): $\delta = 172.3$ (C1'), 166.7 (Ph*C*(O)NHR), 166.4 (C1), 145.4 (C5), 143.9 (C3), 140.1 (Ar), 134.7 (C23), 134.5 (Ar), 134.2 (C16), 133.7 (C11), 132.9 (C25), 132.5 (Ar), 130.4 (C24), 129.4 (C10), 129.23 (2C, Ar), 129.17 (2C, Ar), 129.1 (C15), 128.3 (Ar), 127.8 (C4), 127.6 (2C, Ar), 127.3 (2C, Ar), 118.1 (C26), 117.4 (C2), 79.8 (C13), 78.4 (C7), 76.9 (C21), 76.2 (C19), 74.5 (C2'), 71.9 (C9), 57.4 (OMe), 55.0 (C3'), 38.0 (C6), 37.6 (2C, C17, C20), 37.5 (C14), 35.5 (C12), 35.4 (C8), 35.0 (C22), 31.7 (C18), 23.3 (Me16), 19.3 (Me22), 18.2 (Me12), 17.5 (Me14), 11.90 (Me18), 11.85 (Me6), 10.2 ppm (Me20); HRMS (ES$^+$): *m*/*z*: calcd for $C_{50}H_{68}NO_9$: 826.4894 $[M+H]^+$, found: 826.4907.

Triple hybrid 46: $R_f = 0.51$ (60% EtOAc/petroleum ether); $R_t = 44$ min (2% IPA/hexane); $[\alpha]_{20}^{D} = = +40.9$ ($c = 0.11$ in $CHCl_3$); IR (neat): $\tilde{\nu}_{max} =$ 3421, 2964, 2925, 1710, 1639, 1496, 1454 cm^{-1}; ^{1}H NMR (500 MHz, CD_2Cl_2): $\delta = 7.34$–7.40 (4H, m; Ar), 7.27–7.33 (2H, m; Ar), 6.66 (1H, ddd, $J = 10.4$, 10.8, 16.6 Hz; H25), 6.60 (1H, t, $J = 11.2$ Hz; H3), 6.11 (1H, dd, $J = 6.2$, 15.9 Hz; H5), 6.01 (1H, t, $J = 10.9$ Hz; H24), 5.81 (1H, ddd, $J = 3.2$, 8.6, 11.9 Hz; H9), 5.68 (1H, dd, $J = 8.9$, 11.2 Hz; H11), 5.52–5.58 (2H, m, H2; NH), 5.26–5.31 (2H, m; H10, H23), 5.20 (1H, d, $J =$ 16.7 Hz; H26a), 5.12 (2H, d, $J = 10.2$ Hz; H26B, H3'), 5.00 (1H, dd, $J =$ 3.5, 8.3 Hz; H21), 4.97 (1H, d, $J = 10.4$ Hz; H15), 4.36 (1H, s; H2'), 3.30 (3H, s; OMe), 3.26–3.28 (1H, m; H7), 3.23 (1H, dd, $J = 2.7$, 9.0 Hz; H13), 3.15 (1H, d, $J = 3.1$ Hz; C2'-O*H*), 3.05–3.09 (2H, m; H19, H22), 2.86 (1H, q, $J = 6.3$ Hz; H6), 2.57 (1H, t, $J = 7.7$ Hz; H12), 2.47 (1H, q, $J = 8.1$ Hz; H14), 2.13–2.20 (2H, m; H17a, H18), 1.95 (1H, dt, $J = 3.8$, 7.8 Hz; H20), 1.74 (3H, s; Me16), 1.66–1.68 (1H, m; H17b), 1.63 (1H, d, $J = 12.7$ Hz; H8a), 1.39 (9H, s; C(CH$_3$)$_3$), 1.34–1.38 (1H, obs m; H8b), 1.13 (3H, d, $J = 6.9$ Hz; Me12), 1.10 (3H, d, $J = 6.9$ Hz; Me20), 1.05 (3H, d, $J = 6.9$ Hz; Me6), 1.00 (6H, t, $J = 7.1$ Hz; Me14, Me22), 0.71 ppm (3H, d, $J = 6.1$ Hz; Me18); ^{13}C NMR (125 MHz, CD_2Cl_2): $\delta = 172.2$ (C1'), 166.4 (C1), 155.7 (*t*BuO*C*(O)NHR), 145.1 (C5), 143.9 (C3), 140.8 (Ar), 134.7 (C23), 134.1 (C16), 133.3 (C11), 132.9 (C25), 130.5 (C24), 129.4 (C10), 129.2 (Ar), 129.1 (C15), 128.1 (C4), 127.7 (Ar), 126.9 (Ar), 118.2 (C26), 117.5 (C2), 80.3 (*C*Me$_3$), 79.9 (C13), 78.4 (C7), 76.9 (C21), 76.4 (C19), 74.6 (C2'), 71.6 (C9), 57.5 (OMe), 56.4 (C3<'), 37.8 (C6), 37.7 (C17), 37.6 (C20), 37.5 (C14), 35.4 (C12), 35.0 (2C, C8, C22), 31.7 (C18), 28.6 (3C, C*Me*$_3$), 23.4 (Me16), 19.3 (Me14), 18.2 (Me12), 17.5 (Me22), 11.8 (Me18), 11.6 (Me6), 10.1 ppm (Me20); HRMS (ES$^+$): *m*/*z*: calcd for $C_{48}H_{72}NO_{10}$: 822.5156 $[M+H]^+$, found: 822.5185.

Acknowledgements

Financial support was provided by the EPSRC, AstraZeneca (CASE award to N.M.G.), and the NIH (grant no. R56 CA093455). We thank Dr. J. Fernando Díaz (CSIC, Madrid) for providing AutoDock 3D structures and the figure of the lowest energy conformation of discodermolide in D_2O, Dr. J. Leonard (AstraZeneca) for helpful discussions, Dr. S. Mickel (Novartis) for the gift of chemicals, T. Fujita (Prof. Nakamura's group, University of Tokyo) for the preparation of β-lactams **29** and **30**, Dr R. Paton (Cambridge) for modeling advice, T. Pitts and P. Linley (HBOI) for biological assays, and the EPSRC Swansea Mass Spectrometry Service for mass spectra.

[1] a) F. E. Koehn, G. T. Carter, *Nat. Rev. Drug Discovery* **2005**, *4*, 206; b) M. S. Butler, *Nat. Prod. Rep.* **2008**, *25*, 475; c) D. J. Newman, G. M. Cragg, *J. Nat. Prod.* **2007**, *70*, 461; d) I. Paterson, E. A. Anderson, *Science* **2005**, *310*, 451; e) G. M. L. Cragg, D. G. I. Kingston, D. J. Newman, *Anticancer Agents From Natural Products*, Taylor&-Francis, Boca Raton, **2005**.

[2] a) E. Hamel, *Med. Chem. Rev.* **1996**, *16*, 207; b) K. H. Altmann, J. Gertsch, *Nat. Prod. Rep.* **2007**, *24*, 327.

[3] K. C. Nicolaou, W. M. Dai, R. K. Guy, *Angew. Chem.* **1994**, *106*, 38; *Angew. Chem. Int. Ed. Engl.* **1994**, *33*, 15.

[4] P. B. Schiff, J. Fant, S. B. Horwitz, *Nature* **1979**, *277*, 665.

[5] F. Gueritte-Voegelein, D. Guenard, F. Lavelle, M. T. Le Goff, L. Mangatal, P. Potier, *J. Med. Chem.* **1991**, *34*, 992.

[6] G. A. Orr, P. Verdier-Pinard, H. McDaid, S. B. Horwitz, *Oncogene* **2003**, *22*, 7280.

[7] J. T. Hunt, *Mol. Cancer Ther.* **2009**, *8*, 275.

[8] a) S. P. Gunasekera, M. Gunasekera, R. E. Longley, G. K. Schulte, *J. Org. Chem.* **1990**, *55*, 4912; b) E. Ter Haar, R. J. Kowalski, E. Hamel, C. M. Lin, R. E. Longley, S. P. Gunasekera, H. S. Rosenkranz, B. W. Day, *Biochemistry* **1996**, *35*, 243; c) R. J. Kowalski, P. Giannakakou, S. P. Gunasekera, R. E. Longley, B. W. Day, E. Hamel, *Mol. Pharmacol.* **1997**, *52*, 613.

[9] a) G. R. Pettit, Z. A. Cichacz, F. Goa, M. R. Boyd, J. M. Schmidt, *J. Chem. Soc., Chem. Commun.* **1994**, 1111; b) R. A. Isbrucker, J. Cummins, S. A. Pomponi, R. E. Longley, A. E. Wright, *Biochem. Pharmacol.* **2003**, *66*, 75; c) I. Paterson, R. Britton, O. Delgado, A. E. Wright, *Chem. Commun.* **2004**, 632.

[10] R. M. Buey, E. Calvo, I. Barasoain, O. Pineda, M. C. Edler, R. Matesanz, G. Cerezo, C. D. Vanderwal, B. W. Day, E. J. Sorensen, J. A. Lopez, J. M. Andreu, E. Hamel, J. F. Díaz, *Nat. Chem. Biol.* **2007**, *3*, 117.

[11] R. M. Buey, I. Barasoain, E. Jackson, A. Meyer, P. Giannakakou, I. Paterson, S. Mooberry, J. M. Andreu, J. F. Díaz, *Chem. Biol.* **2005**, *12*, 1269.

[12] a) S. Honore, K. Kamath, D. Braguer, S. B. Horwitz, L. Wilson, C. Briand, M. A. Jordan, *Cancer Res.* **2004**, *64*, 4957; b) G. S. Huang, L. L. Barcons, B. S. Freeze, A. B. Smith III, G. L. Goldberg, S. B. Horwitz, H. M. McDaid, *Clin. Cancer Res.* **2006**, *12*, 298.

[13] For reviews on discodermolide and its analogues, see: a) G. J. Florence, N. M. Gardner, I. Paterson, *Nat. Prod. Rep.* **2008**, *25*, 342; b) I. Paterson, G. J. Florence, *Top. Curr. Chem.* **2009**, *286*, 73; c) A. B. Smith III, B. S. Freeze, *Tetrahedron* **2008**, *64*, 261.

[14] S. J. Mickel, D. Niederer, R. Daeffler, A. Osmani, E. Kuesters, E. Schmid, K. Schaer, R. Gamboni, W. Chen, E. Loeser, F. R. Kinder, K. Konigsberger, K. Prasad, T. M. Ramsey, O. Repic, R.-M. Wang, G. Florence, I. Lyothier, I. Paterson, *Org. Process Res. Dev.* **2004**, *8*, 122.

[15] a) A. Mita, A. C. Lockhart, T.-L. Chen, K. Bochinski, J. Curtright, W. Cooper, L. Hammond, M. Rothenberg, E. Rowinsky, S. Sharma, *J. Clin. Oncol.* **2004**, *22*, 2025; b) A. Mita, A. Lockhart, T. Chen, *Proc. Am. Soc. Clin. Oncol.* **2004**, *23*, 133.

[16] J. P. Snyder, J. H. Nettles, B. Cornett, K. H. Downing, E. Nogales, *Proc. Natl. Acad. Sci. USA* **2001**, *98*, 5312.

[17] A. A. Alcaraz, A. K. Mehta, S. A. Johnson, J. P. Snyder, *J. Med. Chem.* **2006**, *49*, 2478.

[18] R. Geney, L. Sun, P. Pera, R. J. Bernacki, S. Xia, S. B. Horwitz, C. L. Simmerling, I. Ojima, *Chem. Biol.* **2005**, *12*, 339.
[19] a) S. A. Johnson, A. A. Alcaraz, J. P. Snyder, *Org. Lett.* **2005**, *7*, 5549; b) Y. Yang, A. A. Alcaraz, J. P. Snyder, *J. Nat. Prod.* **2009**, *72*, 422; c) L. Sun, C. Simmerling, I. Ojima, *ChemMedChem* **2009**, *4*, 719.
[20] A. Canales, R. Matesanz, N. M. Gardner, J. M. Andreu, I. Paterson, J. F. Díaz, J. Jiménez-Barbero, *Chem. Eur. J.* **2008**, *14*, 7557.
[21] a) E. Monteagudo, D. O. Cicero, B. Cornett, D. C. Myles, J. P. Snyder, *J. Am. Chem. Soc.* **2001**, *123*, 6929; b) A. B. Smith III, M. J. La Marche, M. Falcone-Hindley, *Org. Lett.* **2001**, *3*, 695; c) V. M. Sánchez-Pedregal, K. Kubicek, J. Meiler, I. Lyothier, I. Paterson, T. Carlomagno, *Angew. Chem.* **2006**, *118*, 7548; *Angew. Chem. Int. Ed.* **2006**, *45*, 7388.
[22] R. W. Hoffmann, *Angew. Chem.* **2000**, *112*, 2134; *Angew. Chem. Int. Ed.* **2000**, *39*, 2054.
[23] A. S. Jogalekar, F. H. Kriel, Q. Shi, B. Cornett, D. Cicero, J. P. Snyder, *J. Med. Chem.* **2010**, *53*, 155.
[24] For dictyostatin analogues, see: a) Y. Shin, N. Choy, R. Balachandran, C. Madiraju, B. W. Day, D. P. Curran, *Org. Lett.* **2002**, *4*, 4443; b) W.-H. Jung, C. Harrison, Y. Shin, J. H. Fournier, R. Balachandran, B. S. Raccor, R. P. Sikorski, A. Vogt, D. P. Curran, B. W. Day, *J. Med. Chem.* **2007**, *50*, 2951; c) I. Paterson, N. M. Gardner, K. G. Poullennec, A. E. Wright, *Bioorg. Med. Chem. Lett.* **2007**, *17*, 2443; d) B. S. Raccor, A. Vogt, R. P. Sikorski, C. Madiraju, R. Balanchandran, K. Montgomery, Y. Shin, Y. Fukui, W.-H. Jung, D. P. Curran, B. W. Day, *Mol. Pharmacol.* **2008**, *73*, 718; e) I. Paterson, N. M. Gardner, K. G. Poullennec, A. E. Wright, *J. Nat. Prod.* **2008**, *71*, 364; f) I. Paterson, N. M. Gardner, E. Guzmán, A. E. Wright, *Bioorg. Med. Chem. Lett.* **2008**, *18*, 6268; g) J. L. Eiseman, L. Bai, W.-H. Jung, G. Moura-Letts, B. W. Day, D. P. Curran, *J. Med. Chem.* **2008**, *51*, 6650; h) I. Paterson, N. M. Gardner, G. J. Naylor, *Pure Appl. Chem.* **2009**, *81*, 169; i) I. Paterson, N. M. Gardner, E. Guzmán, A. E. Wright, *Bioorg. Med. Chem.* **2009**, *17*, 2282; j) W. Zhu, M. Jiménez, W.-H. Jung, D. P. Camarco, R. Balachandran, A. Vogt, B. W. Day, D. P. Curran, *J. Am. Chem. Soc.* **2010**, *132*, 9175.
[25] For a preliminary account, see: I. Paterson, N. M. Gardner, *Chem. Commun.* **2007**, 49.
[26] a) I. Paterson, G. J. Florence, K. Gerlach, J. P. Scott, *Angew. Chem.* **2000**, *112*, 385; *Angew. Chem. Int. Ed.* **2000**, *39*, 377; b) I. Paterson, G. J. Florence, K. Gerlach, J. P. Scott, N. Sereinig, *J. Am. Chem. Soc.* **2001**, *123*, 9535; c) I. Paterson, O. Delgado, G. J. Florence, M. O'Brien, J. P. Scott, N. Sereinig, *J. Org. Chem.* **2005**, *70*, 150; d) I. Paterson, O. Delgado, G. J. Florence, I. Lyothier, J. P. Scott, N. Sereinig, *Org. Lett.* **2003**, *5*, 35.
[27] J. Inanaga, K. Hirata, H. Saeki, T. Katsuki, M. Yamaguchi, *Bull. Chem. Soc. Jpn.* **1979**, *52*, 1989.
[28] M. S. Congreve, E. C. Davison, M. A. M. Fuhry, A. B. Holmes, A. N. Payne, R. A. Robinson, S. E. Ward, *Synlett* **1993**, 663.
[29] A. De Mico, R. Margarita, L. Parlanti, A. Vescovi, G. Piancatelli, *J. Org. Chem.* **1997**, *62*, 6974.
[30] W. C. Still, C. Gennari, *Tetrahedron Lett.* **1983**, *24*, 4405.
[31] E. J. Corey, R. K. Bakshi, S. Shibata, *J. Am. Chem. Soc.* **1987**, *109*, 5551.
[32] I. Paterson, R. Britton, O. Delgado, A. Meyer, K. G. Poullennec, *Angew. Chem.* **2004**, *116*, 4729; *Angew. Chem. Int. Ed.* **2004**, *43*, 4629.
[33] For a preliminary account, see: I. Paterson, G. J. Naylor, A. E. Wright, *Chem. Commun.* **2008**, 4628.
[34] I. Paterson, R. Britton, O. Delgado, N. M. Gardner, A. Meyer, G. J. Naylor, K. G. Poullennec, *Tetrahedron* **2010**, *66*, 6534.
[35] D. A. Evans, K. T. Chapman, E. M. Carreira, *J. Am. Chem. Soc.* **1988**, *110*, 3560.
[36] G. D. Allred, L. S. Liebeskind, *J. Am. Chem. Soc.* **1996**, *118*, 2748.
[37] S. P. Gunasekera, R. E. Longley, R. A. Isbruker, *J. Nat. Prod.* **2002**, *65*, 1830.
[38] W. S. Mahoney, D. M. Brestensky, J. M. Stryker, *J. Am. Chem. Soc.* **1988**, *110*, 291.
[39] This rationalization was substantiated when an attempted reduction of the earlier β-hydroxy ketone with the enantiomeric (*S*)-CBS reagent failed to overturn the selectivity, and continued to generate the 1,3-*anti*-diol as the major diastereomer (4:1 d.r.).
[40] This isomerism of the dienoate had also been observed in the synthesis of 10,11-dihydro dictyostatin **22**. A reversible 1,4-conjugate addition of DMAP being the most likely mechanism. Suitable conditions have since been developed to minimize this side-reaction, as reported in Ref. [34]. For the approach by Curran group's to solving this problem, see Ref. [24j].
[41] For a preliminary account, see: I. Paterson, G. J. Naylor, T. Fujita, E. Guzmán, A. E. Wright, *Chem. Commun.* **2010**, *46*, 261.
[42] a) I. Ojima, I. Habus, M. Zhao, M. Zucco, Y. H. Park, C. M. Sun, T. Brigaud, *Tetrahedron* **1992**, *48*, 6985; b) I. Ojima, C. M. Sun, M. Zucco, Y. H. Park, O. Duclos, S. Kuduk, *Tetrahedron Lett.* **1993**, *34*, 4149; c) R. A. Holton, Eur. Pat. Appl. EP400 971; [*Chem. Abstr.* **1991**, *114*, 164568q].
[43] Prepared by adapting the method of Farina et al., see V. Farina, S. I. Hauck, D. G. Walker, *Synlett* **1992**, 761.